Evaluating beta-tubulin variants as predictors of benzimidazole resistance across *Caenorhabditis* nematodes

Amanda O. Shaver[1]*, Ryan McKeown[2]*, Joyce M. Reyes Otero[3], J.B. Collins[1], Daniel W. Hogan[4], James S. Fraser[4], Stephen M. Dreyer[5], Erik J. Ragsdale[5], and Erik C. Andersen[1]

[1] Dept. of Biology, Johns Hopkins University, Mudd Hall 144, 3400 N. Charles Street, Baltimore, Maryland 21218
[2] Dept. of Molecular Biosciences, Northwestern University, 2205 Tech Dr, Evanston, Illinois 60208
[3] Dept. of Biology, University of Puerto Rico, CX33+QM7, San Juan, 00925, Puerto Rico t
[4] Dept. of Bioengineering and Therapeutic Sciences, University of California San Francisco, 600 16th St., Genentech Hall Room S472E, San Francisco, CA 94143
[5] Dept. of Biology, Indiana University, Biology Building, Rm. 142, 1001 East Third St., Bloomington, Indiana, 47405
* These authors contributed equally.

Corresponding author:
Erik C. Andersen
Johns Hopkins University
Department of Biology
3400 N. Charles St.
Bascom UTL 383
Baltimore, MD 21218
410-516-1282
erik.andersen@gmail.com

ORCIDs and emails:
Amanda O. Shaver: 0000-0002-2910-1505, amanda.shaver@jhu.edu, amandaoshaver@gmail.com
Ryan McKeown: 0000-0003-3570-2494, ryanmckeown2021@u.northwestern.edu
Joyce M. Reyes Otero: 0009-0002-5039-4434, joyce.reyes2@upr.edu
J.B. Collins: 0000-0003-0808-5216, jcolli95@jh.edu
Daniel W. Hogan: 0000-0003-3375-408X, Daniel.Hogan@ucsf.edu
James S. Fraser: 0000-0002-5080-2859, jfraser@fraserlab.com
Stephen Dreyer: 0000-0003-3900-6031, stdreyer@iu.edu
Erik J. Ragsdale: 0000-0002-9367-8552, ragsdale@iu.edu
Erik C. Andersen: 0000-0003-0229-9651, erik.andersen@gmail.com

Short title: Beta-tubulin mediated benzimidazole resistance

Keywords: *C. elegans*, *C. briggsae*, *C. tropicalis*, beta-tubulin, benzimidazole resistance

ABSTRACT

Benzimidazoles, a widely used class of anthelmintic drugs, target beta-tubulin, disrupt microtubule formation, and delay nematode development. In parasitic nematodes, mutations in beta-tubulin genes are predicted to inhibit benzimidazole binding and are associated with resistance. In the free-living nematode *Caenorhabditis elegans*, loss-of-function mutations in the beta-tubulin gene *ben-1* cause benzimidazole resistance. Although several beta-tubulin mutations serve as established markers of resistance, the prediction of the effects of novel variants in different nematode species remains challenging. Here, we identified novel beta-tubulin variants predicted to confer benzimidazole resistance across wild strains in three *Caenorhabditis* species: *C. elegans*, *Caenorhabditis briggsae*, and *Caenorhabditis tropicalis*. The three *Caenorhabditis* species are experimentally tractable, have characterized beta-tubulin gene complements, and defined natural niches, which allowed us to identify variants in beta-tubulin genes and test which variants are associated with resistance. We hypothesized that, if these species experienced similar selective pressures, they would evolve resistance to benzimidazoles by mutations in a beta-tubulin gene (*tbb-1*, *tbb-2*, *mec-7*, *tbb-4*, and *ben-1*). In the three *Caenorhabditis* species, we tested all strains harboring variants in the five conserved beta-tubulin genes for benzimidazole resistance. In *C. elegans*, we found that a heterogeneous set of variants in *ben-1* were associated with resistance. By contrast, only two variants in *C. briggsae ben-1* (W21stop and Q134H) were associated with resistance. *C. tropicalis* was distinct from the other two species, where no strains with variants in any beta-tubulin gene were resistant. We generated deletions of *ben-1* in *C. briggsae* and *C. tropicalis* and confirmed that loss of *ben-1* confers resistance in both species. Our findings reveal species-specific patterns of beta-tubulin-mediated benzimidazole resistance and emphasize that prediction of variants in beta-tubulin genes alone is not sufficient to predict resistance, especially across diverse nematode species.

AUTHOR SUMMARY

Mutations in beta-tubulin genes have been associated with benzimidazole resistance across nematode species, yet predicting novel resistance variants remains challenging. Using wild strains from three *Caenorhabditis* species, we identified strains with variants in beta-tubulin genes and tested each strain for benzimidazole resistance. In *C. elegans,* a diverse set of loss-of-function variants in *ben-1* were associated with resistance. Whereas in *C. briggsae*, only two *ben-1* alleles were associated with resistance, suggesting selection acts differently in this species despite a similar niche as *C. elegans*. *C. tropicalis* had no strains with beta-tubulin variants that were resistant. Our results highlight species-specific patterns of benzimidazole resistance.

71 **INTRODUCTION**

72 Global control of parasitic nematode infections relies on the efficacy of a small arsenal of anthelmintic
73 drugs, including benzimidazoles (BZs) [1]. BZs are a widely used class of anthelmintic drugs that inhibit the
74 polymerization of microtubules [2–4] and delay nematode development [5]. Although BZs are essential to human
75 and veterinary health, resistance is prominent in parasitic nematode populations [6,7]. In clade V nematodes
76 (*e.g.*, *Ancylostoma caninum*, *Ancylostoma duodenale*, *Caenorhabditis elegans*, *Haemonchus contortus*, *Necator*
77 *americanus*, *Teladorsagia circumcincta*, and *Trichostrongylus colubriformis*), BZ resistance is associated with
78 mutations in beta-tubulin genes [8–16].

79 Among parasitic nematodes, BZ resistance has been best characterized in the small ruminant parasite
80 *H. contortus* [17]. The *H. contortus* genome contains four genes that encode beta-tubulins (*tbb-isotype-1*, *tbb-*
81 *isotype-2*, *tbb-isotype-3*, and *tbb-isotype-4*), where each encoded protein has a phenylalanine at position 200,
82 which is thought to confer binding to BZs [18]. In field populations of *H. contortus*, BZ resistance has been
83 associated historically with three canonical missense variants (F167Y, E198A, and F200Y) in *tbb-isotype-1* [19–
84 22]. Recently, additional novel missense variants in *tbb-isotype-1* have been associated with *H. contortus* BZ
85 resistance (*e.g.*, E198I, E198K, E198T, and E198stop) [23] These newly described missense variants in *tbb-*
86 *isotype-1* are hypothesized to disrupt BZ binding, without causing loss-of-function (LoF). Given the high
87 expression of *tbb-isotype-1*, it is likely an essential beta-tubulin in *H. contortus [18]*. By contrast, *tbb-isotype-2*
88 LoF alleles have been identified in highly resistant *H. contortus* populations [24], indicating that it is not an
89 essential gene and does not confer resistance on its own because variants are not observed in resistant *H.*
90 *contortus* populations [18]. The other two beta-tubulin genes are expressed at low levels and have not been
91 associated with BZ resistance [18]. The beta-tubulin genes and alleles involved in BZ resistance suggest that
92 specific variants that prevent or reduce BZ binding can be tolerated, whereas complete loss of essential beta-
93 tubulin genes cannot.

94 Unlike *H. contortus*, the free-living model nematode species *C. elegans* has six beta-tubulin genes (*tbb-*
95 *1*, *tbb-2*, *mec-7*, *tbb-4*, *ben-1*, and *tbb-6*) [25]. LoF mutations in *ben-1*, an ortholog of *H. contortus tbb-isotype-1*
96 and *tbb-isotype-2* [18], confer BZ resistance [26]. Additionally, a heterogeneous set of LoF variants in *ben-1*
97 identified in *C. elegans* wild strains cause natural BZ resistance in this species [14]. The ability to maintain wild-

98 type growth despite the loss of *ben-1* is likely explained by functional redundancy among beta-tubulin genes
99 [27]. Previous studies have demonstrated that *Cel-tbb-1* and *Cel-tbb-2* act redundantly for viability [28–30] and
100 for movement, body morphology, and growth [31]. In *C. elegans*, *tbb-1* and *tbb-2* are the most broadly and highly
101 expressed beta-tubulin genes, whereas *ben-1* expression is restricted largely to neurons, specifically cholinergic
102 and glutamatergic neurons [25,32]. Consistent with this pattern, cell-specific rescue experiments demonstrated
103 that *ben-1* acts in cholinergic and GABAergic neurons to confer BZ susceptibility, suggesting that these neurons
104 are key sites of BZ action [33]. Of the six *C. elegans* beta-tubulins, only MEC-7, TBB-4, and BEN-1 contain a
105 phenylalanine at position 200, the residue associated with BZ binding in *H. contortus*, whereas TBB-1 and TBB-
106 2 contain tyrosine at this position and are predicted not to bind BZs. Together, these findings illustrate how loss
107 of a *C. elegans* beta-tubulin that can bind BZs causes resistance because other beta-tubulin genes are
108 functionally redundant for viability and do not bind BZs.

109 The recurrent association of beta-tubulin variants with BZ resistance in clade V parasitic and free-living
110 nematodes suggests the hypothesis that resistance might be predictable across species. However, the reliability
111 of beta-tubulin variants as predictors of BZ resistance across nematode species is unknown. This hypothesis is
112 difficult to test directly in parasitic nematode species because of their host-dependent life cycles, poorly
113 annotated reference genomes, and limited molecular and genetic tools [34,35]. By contrast, the availability of
114 high-quality genomic data for hundreds of wild strains [36] and the laboratory tractability of the free-living
115 *Caenorhabditis* nematode species, *C. elegans*, *Caenorhabditis briggsae*, and *Caenorhabditis tropicalis*, provide
116 an opportunity to test predictions of beta-tubulin mediated BZ resistance in the *Caenorhabditis* genus.
117 Establishing and interrogating patterns of repeated evolution in these three free-living species would provide a
118 mechanistic framework to anticipate resistance-associated variants in beta-tubulin genes across other clade V
119 nematode species, including parasitic nematodes where direct experimental validation of resistance
120 mechanisms remains a challenge.

121 Using the global natural diversity of *C. elegans*, *C. briggsae*, and *C. tropicalis*, we assessed variation in
122 the beta-tubulin genes *tbb-1*, *tbb-2*, *mec-7*, *tbb-4*, and *ben-1* and identified high-impact variants (*i.e.*, single
123 nucleotide variants (SNVs), small insertions or deletions (INDELs), and structural variants (SVs) predicted to
124 disrupt beta-tubulin function and confer BZ resistance. Because *ben-1* is the primary driver of BZ resistance in

125 *C. elegans*, we used an established high-throughput larval development assay (HTLDA) to expose strains with
126 novel *ben-1* variants to the highly used BZ, albendazole (ABZ). In *C. elegans*, strains harboring seven of nine
127 novel *Cel-ben-1* variants were resistant to ABZ, adding more alleles hypothesized to confer resistance in this
128 species. By contrast, strains harboring only two of the eight unique *Cbr-ben-1* variants (W21stop and Q134H)
129 were resistant to ABZ. *C. tropicalis* was distinct from the other two species, where no strains with variants in *ben-*
130 *1* were resistant to ABZ. To validate the roles of *Cbr-ben-1* and *Ctr-ben-1* in BZ resistance, we generated deletion
131 alleles and confirmed that loss of *ben-1* confers resistance in both *C. briggsae* and *C. tropicalis*. Fecundity assays
132 showed that a loss of *Cbr-ben-1* did not affect *C. briggsae* fitness, whereas a deletion of *Ctr-ben-1* significantly
133 reduced fecundity in *C. tropicalis*. Because *ben-1* variants could not always predict ABZ resistance, we tested
134 whether strains harboring high-impact variants in the other four conserved beta-tubulin genes were resistant to
135 ABZ. Strains with variants in *tbb-1*, *tbb-2*, *mec-7*, and *tbb-4* were not resistant to ABZ in any of the three
136 *Caenorhabditis* species, indicating that *ben-1* is the primary beta-tubulin that confers resistance. The species-
137 specific patterns of beta-tubulin-mediated BZ resistance might reflect species-specific selection pressures, such
138 as exposure to natural BZs, and can shape the evolution of beta-tubulin-mediated resistance. The identification
139 of alleles associated with BZ resistance in experimentally tractable species establishes a framework to predict
140 beta-tubulin variants associated with resistance in other clade V nematodes.
141

142 **RESULTS**

143 **Strains with variants or expression differences in *ben-1* were predicted to be ABZ resistant**

144 To predict ABZ resistant strains in the three *Caenorhabditis* species, we identified high-impact variants
145 (SNVs, INDELs, or SVs) in *ben-1* (see *Materials and Methods*). In a set of 611 *C. elegans* wild strains [36], we
146 identified 65 strains with 33 unique high-impact variants in *ben-1* (**S1 Table**). Of the 33 variants, 24 were
147 previously phenotyped and 20 were associated with ABZ resistance (**S1A Fig.**) [14,37]. In 641 *C. briggsae* wild
148 strains, 22 strains with eight unique high-impact variants in *ben-1* were identified (**S2 Table**). In a set of 518 *C.*
149 *tropicalis* wild strains, only two strains with unique high-impact variants in *ben-1* were identified (**S3 Table**).

150 Next, because low *ben-1* expression was previously correlated with ABZ resistance in *C. elegans* wild
151 strains [38], we evaluated whether *ben-1* expression levels were predictive of ABZ responses in *C. elegans.* We

152 assessed the relationship between the expression of *ben-1* [38] and ABZ responses in 180 *C. elegans* wild
153 strains [14,37] (*p*-value = 5.16e-16, r^2= 0.344). We hypothesized that low *ben-1* expression could contribute to
154 ABZ resistance in *C. briggsae* and *C. tropicalis*, but expression data from wild strains in these species have yet
155 to be collected.

156 Altogether, we identified nine novel variants in *Cel-ben-1* (E3stop, Y50C, P80S, VDN113N, Q131L,
157 frameshift 319, frameshift 368, stop445S, and a duplication) (**S1 Table**), one strain with low *Cel-ben-1*
158 expression, eight variants in *Cbr-ben-1* (W21stop, V91I, Q94K, D128E, Q134H, S218L, M299V, and R359H)
159 (**S2 Table**), and two variants in *Ctr-ben-1* (P80T and R121Q) (**S3 Table**) to test for ABZ resistance. In addition
160 to these selected strains, we also selected *C. briggsae* and *C. tropicalis* strains that lacked high-impact variants
161 in beta-tubulin genes but were closely related to strains with variants (**S2 Fig., S3 Fig., and S4 Table**). The
162 strains with no high-impact variants in any beta-tubulin gene might control for differences in wild strain genetic
163 backgrounds.

164

165 **High-throughput larval development assays (HTLDAs) reveal species-specific associations between**
166 ***ben-1* variation and ABZ resistance**

167 Nematodes grow longer as they progress through development, and BZs slow this progression [14–
168 16,27,37]. A longer animal length (*i.e.*, larger animals) corresponds to increased ABZ resistance, and a shorter
169 animal length (*i.e.*, smaller animals) corresponds to increased ABZ sensitivity. To evaluate the effects of ABZ on
170 animal length (a proxy for development), we used image-based HTLDAs to expose all *C. elegans*, *C. briggsae*,
171 and *C. tropicalis* wild strains with novel high-impact variants in *ben-1* or low *ben-1* expression (*i.e.*, predicted
172 resistant strains) to control (DMSO) (**S4 Fig., S5 Fig., and S6 Fig.**) and drug (ABZ) conditions (**S7 Fig., S8 Fig.,**
173 **and S9 Fig.**) (see *Materials and Methods*). The assay included 48 replicates per strain with five to 30 animals
174 per replicate in DMSO or ABZ conditions. The reported nematode length of each strain is the difference between
175 animal lengths in DMSO and ABZ.

176 To define the role of *ben-1* in BZ response and classify wild strains as BZ resistant, we first obtained or
177 created *ben-1* deletions in the reference strains for each of the three *Caenorhabditis* species. In *C. elegans*, the
178 strain with a *ben-1* LoF variant in the N2 strain background (ECA882) has been used as an ABZ-resistant control

179 previously [14,27,37]. For *C. briggsae* and *C. tropicalis*, we used CRISPR-Cas9 genome editing to generate two
180 independent *ben-1* deletion alleles per species (see *Materials and Methods*). In *C. briggsae*, deletions of *Cbr-*
181 *ben-1* were created in the AF16 reference strain background (ECA3953 and ECA3954) (**S10 Fig. and S5 Table**).
182 In *C. tropicalis*, deletions of *Ctr-ben-1* were created in the NIC58 reference strain background (ECA4247 and
183 ECA4248) (**S11 Fig. and S5 Table**). All deletions of *ben-1* in each of the three *Caenorhabditis* species conferred
184 high levels of ABZ resistance (**S12 Fig. and S13 Fig.**). Wild strains were then classified as resistant using a
185 threshold where the median animal lengths after ABZ exposure were no more than two SD below the median
186 animal length of the species-specific *ben-1* deletion strain.

187 In *C. elegans*, seven of the nine strains with *ben-1* variants showed minimal developmental delays after
188 exposure to ABZ, a phenotype similar to loss of *ben-1*, and were classified as resistant (**Fig. 1**). The two
189 remaining strains with *ben-1* variants (P80S, stop445S) and the strain with low *ben-1* expression were not
190 strongly resistant to ABZ. The P80S variant might partially alter *ben-1* function, causing a moderate resistance
191 phenotype. In stop445S, the normal stop codon was replaced with a serine. This variant likely does not affect
192 *ben-1* function because position 445 is at the end of the BEN-1 protein, and only four amino acid residues (NRKL)
193 are added beyond the wild-type stop codon. Finally, the strain with low *ben-1* expression and no high-impact
194 variants in *ben-1* (JU1581) was sensitive to ABZ, indicating that the selected threshold of *ben-1* expression
195 (≥3.75 TPM) still retained strains with adequate *ben-1* function. Overall, natural allelic variation in *Cel-ben-1* is
196 associated with BZ resistance, recapitulating previous findings that BZ resistance is associated with a diverse
197 set of LoF variants in *Cel-ben-1* [14,27,31,37].

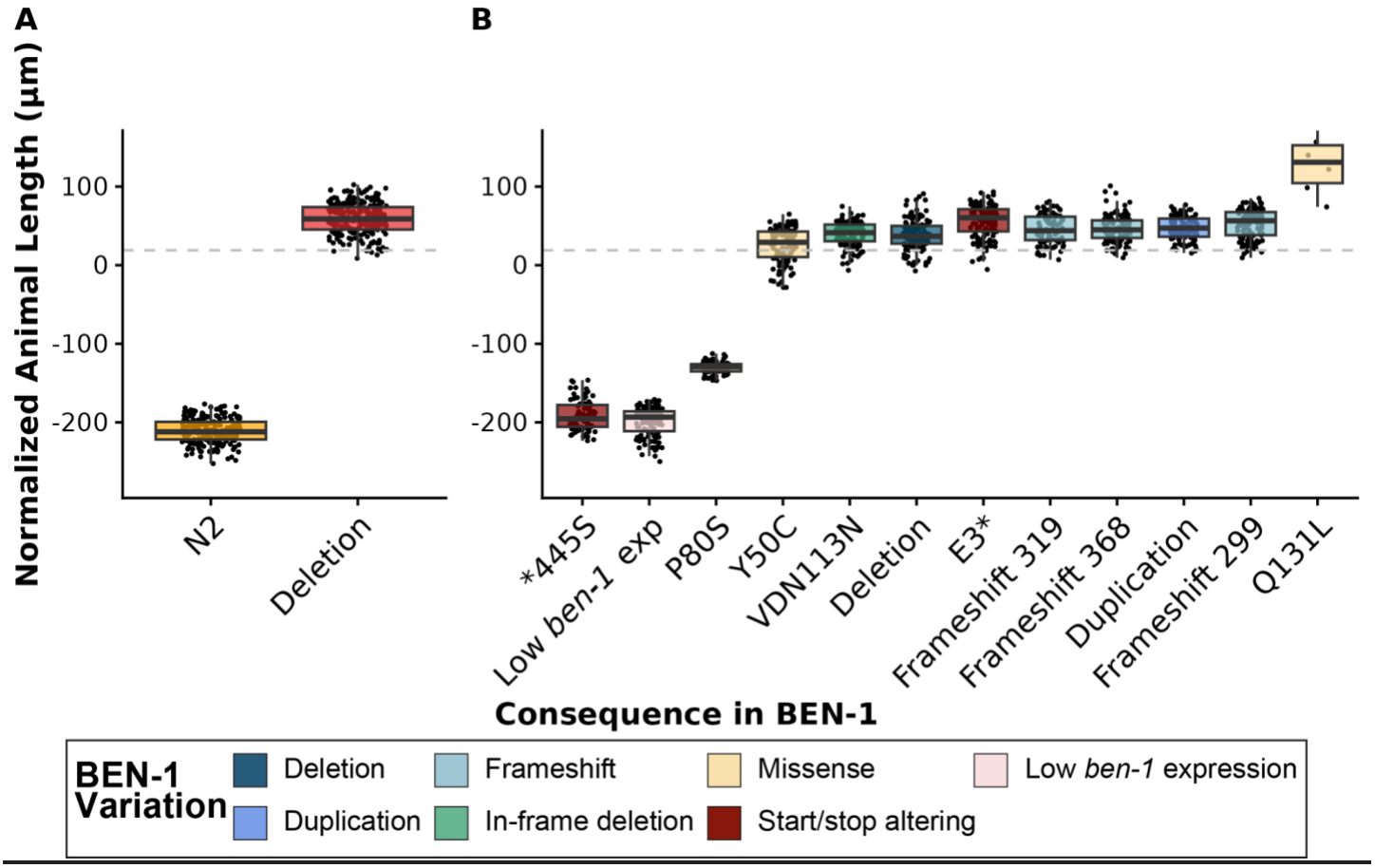

Fig 1. High-throughput larval development assays in the presence of albendazole for *C. elegans* strains with unique high-impact variants in BEN-1.
The regressed median animal length values for populations of nematodes grown in 30 µM albendazole (ABZ) are shown on the y-axis. Each point represents the normalized median animal length value of a well containing approximately 5-30 animals. Strains are sorted by their relative resistance to ABZ based on median animal length. Data are shown as Tukey box plots with the median as a solid horizontal line, and the top and bottom of the box representing the 75th and 25th quartiles, respectively. The top whisker is extended to the maximum point that is within the 1.5 interquartile range from the 75th quartile. The bottom whisker is extended to the minimum point that is within the 1.5 interquartile range from the 25th quartile. The gray dashed line marks the *C. elegans* resistance threshold, defined as two standard deviations below the mean of the *ben-1* deletion strain in the N2 reference strain background. Results for **(A)** the N2 reference strain (orange) and a strain with a *ben-1* deletion in the N2 background (red), and **(B)** all wild *C. elegans* strains with unique high-impact variants in *ben-1* are sorted by their relative resistance to ABZ based on median animal length. Wild *C. elegans* strains are colored by beta-tubulin variant status.

In *C. briggsae*, we performed HTLDAs on the AF16 reference strain (ABZ sensitive), two *ben-1* deletion strains (ECA3953 and ECA3954) (ABZ resistant), 11 strains with eight unique variants in *ben-1*, and 13 strains genetically related to strains with *ben-1* variants in DMSO (control) (**S5 Fig.**) and ABZ conditions (**Fig. 2, S8 Fig., and S12 Fig.**). Of the 11 strains with *Cbr-ben-1* variants, only two strains with unique variants in BEN-1 (Q134H and W21stop) were ABZ resistant (**Fig. 2**). The Q134H amino acid change has been associated with ABZ

220 resistance in *A. caninum* and validated in *C. elegans* [11]. An early stop gain at position 21 is predicted to cause
221 the premature termination of protein synthesis and LoF. Of all the assayed strains with variants in BEN-1, six
222 (V91I, Q94K, D128E, S218L, M299V, and R359H) were not resistant to ABZ. Additionally, eleven *C. briggsae*
223 strains were exposed to a maximum concentration of 120 μM ABZ, where only two strains with the variants
224 Q134H and W21stop were resistant at these higher concentrations (**S14 Fig.**). Overall, because only one of the
225 seven missense variants was associated with ABZ resistance, we could not reliably predict *C. briggsae* ABZ
226 resistance based on the presence of a missense variant alone. To evaluate the potential fitness consequences
227 of *ben-1* LoF alleles, fecundity assays were performed between the AF16 reference strain and the two strains
228 with a loss of *ben-1* in the AF16 background (ECA3953 and ECA3954) (**S15A Fig. and S6 Table**). We found no
229 significant differences in fecundity between the three strains, indicating that a loss of *ben-1* does not affect fitness
230 in this species. These results indicate that, although a loss of *Cbr-ben-1* confers ABZ resistance with no fitness
231 detriment, ABZ resistance associated with *Cbr-ben-1* variants is uncommon.
232

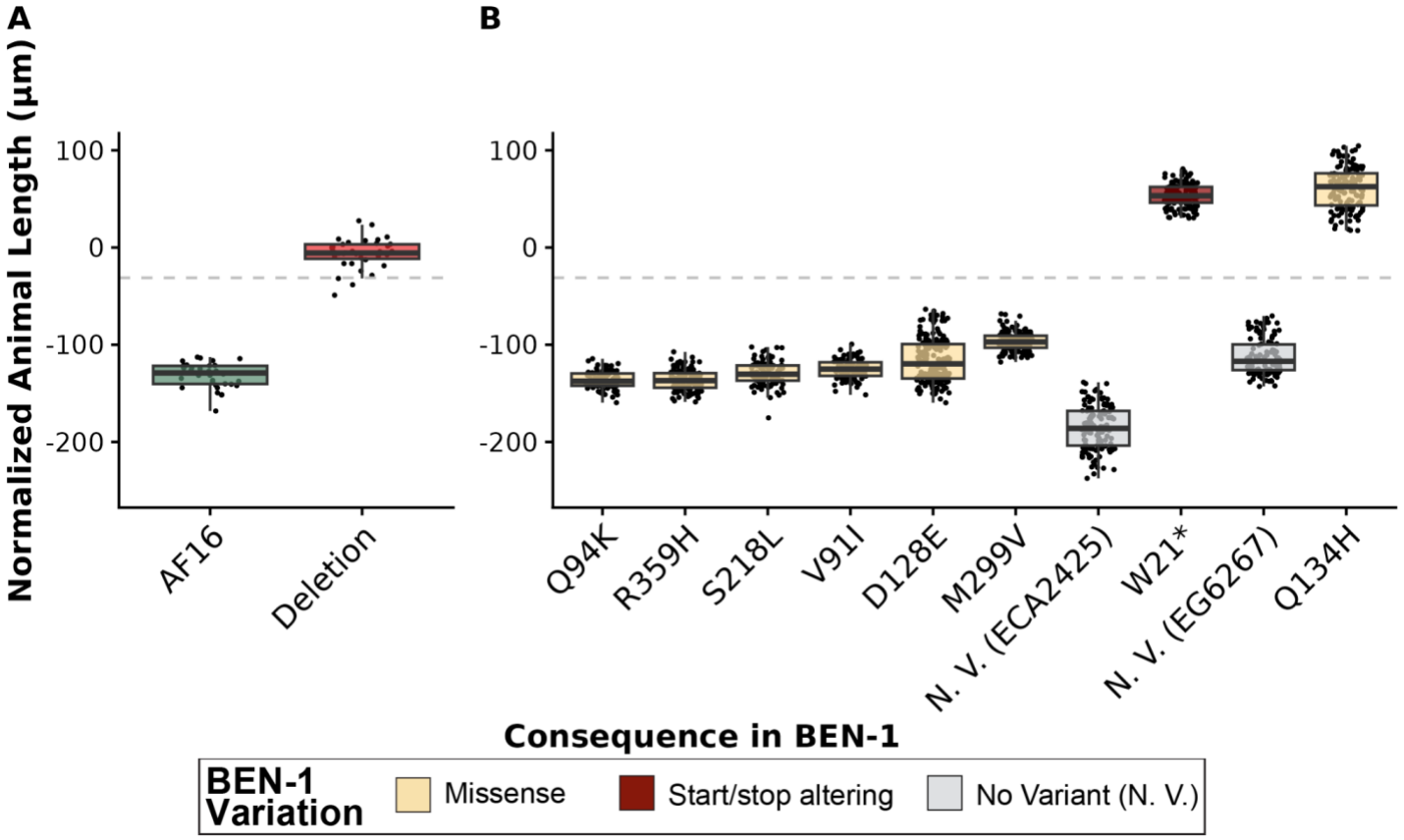

233
234 **Fig 2. High-throughput larval development assays in the presence of albendazole for *C. briggsae* strains**
235 **with unique high-impact variants in BEN-1.**

236 The regressed median animal length values for populations of nematodes grown in 30 μM albendazole (ABZ)
237 are shown on the y-axis. Each point represents the normalized median animal length value of a well containing
238 approximately 5-30 animals. Data are shown as Tukey box plots with the median as a solid horizontal line, and
239 the top and bottom of the box representing the 75th and 25th quartiles, respectively. The top whisker is extended
240 to the maximum point that is within the 1.5 interquartile range from the 75th quartile. The bottom whisker is
241 extended to the minimum point that is within the 1.5 interquartile range from the 25th quartile. The gray dashed
242 line marks the *C. briggsae* resistance threshold, defined as two standard deviations below the mean of the *ben-*
243 *1* deletion strain in the AF16 reference strain background. Results for **(A)** the AF16 reference strain (green) and
244 a strain with a *ben-1* deletion in the AF16 background (red), and **(B)** all wild *C. briggsae* strains with unique high-
245 impact variants in *ben-1* are sorted by their relative resistance to ABZ based on median animal length. No variant
246 (N. V.) strains (gray) paired with strains that have a high-impact variant in *ben-1* that pass the resistance
247 threshold are shown alongside each corresponding strain with a high-impact variant in *ben-1*. Wild *C. briggsae*
248 strains are colored by beta-tubulin variant status.
249

250 In *C. tropicalis*, we performed HTLDAs on the reference strain NIC58 (ABZ sensitive), two independent
251 deletions of *Ctr-ben-1* (ECA4247 and ECA4248) (ABZ resistant), two *C. tropicalis* strains with variants in *ben-1*
252 (P80T and R121Q), and two strains genetically related to *ben-1* variant strains in DMSO (**S6 Fig.**) and ABZ
253 conditions (**Fig. 3 and S9 Fig.**). We found that all *C. tropicalis* wild strains displayed ABZ sensitivity, indicating
254 that P80T and R121Q are not associated with ABZ resistance (**Fig. 3**). Additionally, all tested wild strains were
255 exposed to a maximum concentration of 120 μM ABZ, and none of the strains displayed resistance at these
256 higher concentrations (**S16 Fig.**). Finally, to evaluate the potential fitness consequences caused by a loss of
257 *ben-1*, fecundity assays were performed between the NIC58 reference strain and the two strains with a loss of
258 *ben-1* in the NIC58 background (ECA4247 and ECA4248) (**S15B Fig. and S7 Table**). We found that a deletion
259 of *ben-1* caused a significant reduction in fecundity in *C. tropicalis*. The fitness defect caused by a loss of *ben-1*
260 could explain the absence of naturally occurring *ben-1* variants in wild *C. tropicalis* strains, suggesting that
261 *C. tropicalis* is unlikely to acquire natural *ben-1* variants that confer ABZ resistance without strong selection. If
262 ABZ resistance is present in *C. tropicalis* wild strains, its genetic basis remains unknown and involves factors
263 distinct from *ben-1*.

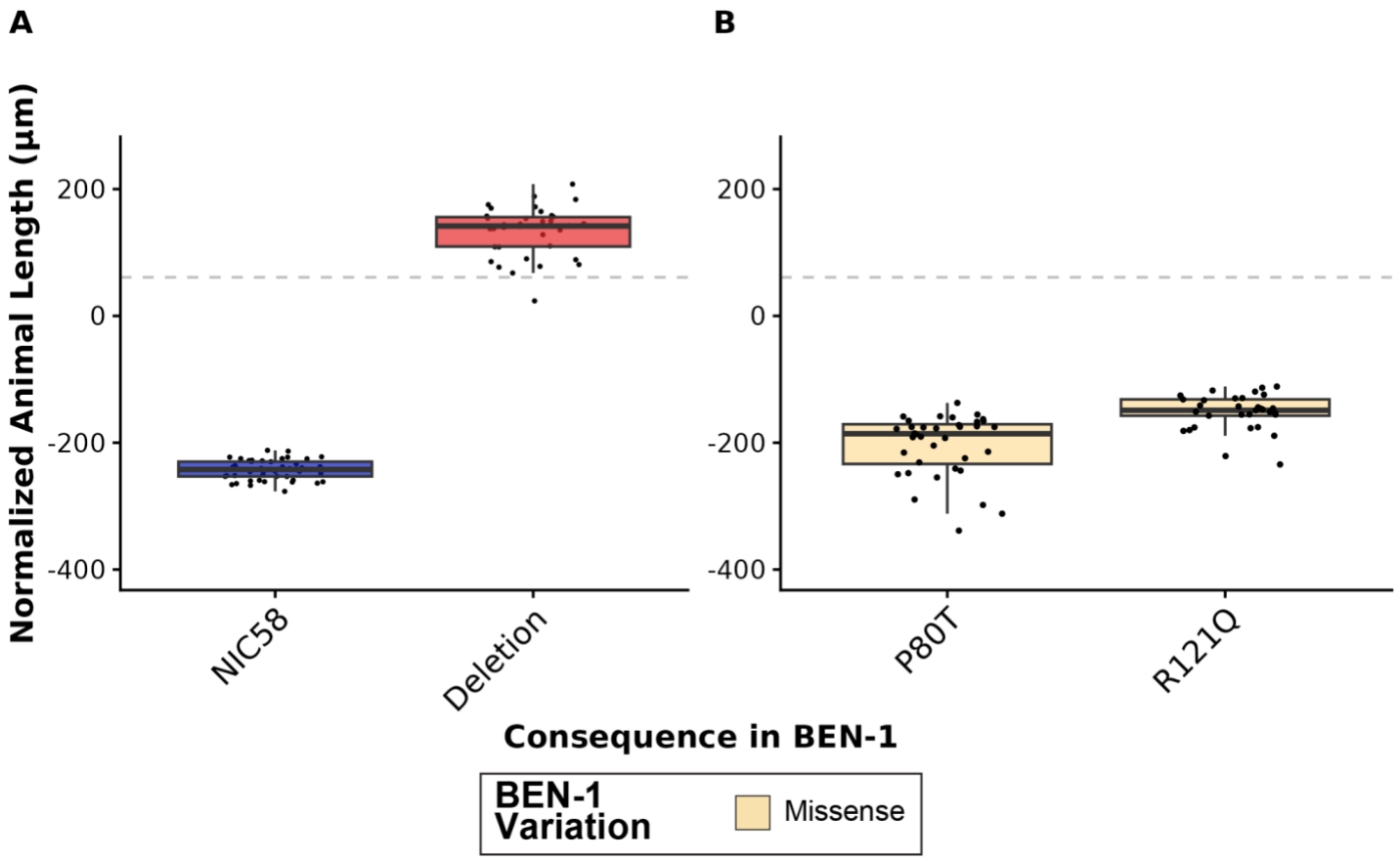

Fig 3. High-throughput larval development assays in the presence of albendazole for *C. tropicalis* strains with unique high-impact variants in BEN-1.
The regressed median animal length values for populations of nematodes grown in 30 µM albendazole (ABZ) are shown on the y-axis. Each point represents the normalized median animal length value of a well containing approximately 5-30 animals. Strains are sorted by their relative resistance to ABZ based on median animal length. Data are shown as Tukey box plots with the median as a solid horizontal line, and the top and bottom of the box representing the 75th and 25th quartiles, respectively. The top whisker is extended to the maximum point that is within the 1.5 interquartile range from the 75th quartile. The bottom whisker is extended to the minimum point that is within the 1.5 interquartile range from the 25th quartile. The gray dashed line marks the *C. tropicalis* resistance threshold, defined as two standard deviations below the mean of the *ben-1* deletion strain in the NIC58 reference strain background. Results for **(A)** the NIC58 reference strain (blue) and a strain with a *ben-1* deletion in the NIC58 background (red), and **(B)** all wild *C. tropicalis* strains with unique high-impact variants in *ben-1* are sorted by their relative resistance to ABZ based on median animal length. Wild *C. tropicalis* strains are colored by beta-tubulin variant status.

The predicted molecular consequence and severity of *ben-1* variants do not predict BZ resistance

To evaluate whether the predicted molecular consequence and severity of *ben-1* variants were predictive of BZ resistance, we characterized the identities and predicted functional impacts of each amino acid altering variant. We distinguished between alleles that disrupt multiple amino acids (*i.e.*, frameshifts, stop/start altering variants, and SVs) and alleles that affect a single amino acid (*i.e.*, missense alleles). Multi-site alleles were excluded from further analysis because they are predicted to severely disrupt or terminate BEN-1 function,

287 whereas missense alleles might preserve an intact protein and allow interpretation of residue-level effects on BZ
288 interaction.

289 In *C. elegans*, seven unique missense substitutions in BEN-1 were identified, of which five (Y50C, Q131L,
290 S145F, A185P, M275I) were associated with BZ resistance (**S17A Fig.**) [14]. In *C. briggsae*, seven unique
291 missense substitutions in *Cbr*-BEN-1 were identified, but only Q134H was associated with BZ resistance (**S17B**
292 **Fig.**). In *C. tropicalis*, both missense substitutions (P80T and R121Q) were not associated with BZ resistance
293 (**S17C Fig.**). To evaluate if missense variants with larger predicted functional impacts were associated with BZ
294 resistance, we quantified the severity of each substitution using BLOSUM62 and Grantham scores [39,40].
295 BLOSUM scores measure the evolutionary likelihood of observing a specific missense substitution, and
296 Grantham scores measure the physicochemical severity of a substitution. Because *C. elegans* had the most
297 missense variants associated with BZ resistance, we performed a regression analysis of each strain's response
298 to ABZ by the BLOSUM or Grantham scores of the strain's beta-tubulin variant. For *C. elegans*, neither BLOSUM
299 or Grantham scores showed a significant correlation with ABZ response (**S18 Fig.**). By contrast, too few
300 missense variants were associated with BZ resistance among *C. briggsae* and *C. tropicalis* strains to
301 meaningfully interpret BLOSUM or Grantham scores for these species (**S8 Table**). The limited number of
302 missense substitutions among wild strains and the even smaller subset associated with BZ resistance
303 constrained statistical power to evaluate structure-function relationships between naturally occurring beta-tubulin
304 variants and BZ response.

305 Next, we mapped missense variants onto an AlphaFold-predicted BEN-1 protein structure that showed
306 that the five *C. elegans* missense substitutions associated with resistance are located within the core, whereas
307 the two substitutions not associated with resistance (P80S and D404N) are on the protein surface (**S17A Fig.**).
308 By contrast, all *C. briggsae* (except Q134H) and all *C. tropicalis* missense substitutions are on the protein surface
309 and are not associated with resistance (**S17B Fig.**). For structural comparison, we modeled *H. contortus tbb-*
310 *isotype-1* beta-tubulin bound to ABZ, and highlighted the canonical missense variants at positions 167, 198, and
311 200 (**S17D Fig.**), all of which are located within the core of the structure, near the predicted BZ-binding pocket
312 and are associated with resistance (**S17D Fig.**) [18–22,41]. These results suggest that BZ resistance is
313 associated with missense substitutions occurring within the protein core likely affecting the theoretical BZ-binding

314 pocket.

315

316 **Natural variants in *tbb-1*, *tbb-2*, *mec-7*, and *tbb-4* are not associated with ABZ resistance across the three**
317 **free-living *Caenorhabditis* species**

318 Although it has been established that *ben-1* is the primary gene involved in ABZ resistance in *C. elegans*
319 [14,27,37], we know less about the role each beta-tubulin gene plays in *C. briggsae* and *C. tropicalis* ABZ
320 resistance. Therefore, we identified variants in the other four conserved beta-tubulin genes across the three
321 *Caenorhabditis* species. We found no variants in *Cel-tbb-1* or *Cel-tbb-2* in any *C. elegans* wild strains (CaeNDR
322 Release ID: *C. elegans* - 20231213) (**Fig. 4**). However, we did identify strains with one missense variant (A9T)
323 in *Cel-mec-7*, a splice donor variant in *Cel-mec-7*, or one missense variant in *Cel-tbb-4* (Q8H) (**S1 Table**). The
324 strain with a splice donor variant in *Cel-mec-7* also carried a high-impact variant (*445S) in *Cel-ben-1*. We also
325 assessed the relationship between the expression of *Cel-tbb-1*, *Cel-tbb-2*, *Cel-mec-7*, or *Cel-tbb-4* [38] and ABZ
326 responses in 180 wild strains (**S19 Fig.**) [14,37]. In *C. briggsae*, we identified strains with missense variants in
327 *Cbr-tbb-1* (T35A, V64I, A275T, and L377I), *Cbr-tbb-2* (E441A), *Cbr-tbb-4* (A271V), and *Cbr-mec-7* (T136I,
328 N165S, and S338C) (CaeNDR Release ID: *C. briggsae* - 20240129) (**S2 Table**). In *C. tropicalis*, we identified
329 no high-impact variants in *Ctr-tbb-1*, one missense variant in *Ctr-tbb-2* (N89S), two missense variants in *Ctr-*
330 *mec-7* (P80F, D433E), and one missense variant in *Ctr-tbb-4* (A78V) (CaeNDR Release ID: *C. tropicalis* -
331 20231201) (**S3 Table**). Because expression data from *C. briggsae* and *C. tropicalis* wild strains have yet to be
332 collected, we could not test correlations of beta-tubulin gene expression with resistance. We performed HTLDAs
333 under control (DMSO) (**S20 Fig., S21 Fig., and S22 Fig.**) and ABZ conditions (**S23 Fig., S24 Fig., and S25**
334 **Fig.**) on strains in the three *Caenorhabditis* species carrying variants in the conserved beta-tubulin genes *tbb-1*,
335 *tbb-2*, *mec-7*, and *tbb-4*, along with strains genetically related to strains with variants in those beta-tubulin genes.
336 No variants outside of *ben-1* conferred ABZ resistance in any species, indicating that natural missense variants
337 in *tbb-1*, *tbb-2*, *mec-7*, and *tbb-4* are not associated with BZ resistance in the three selfing *Caenorhabditis*
338 species.

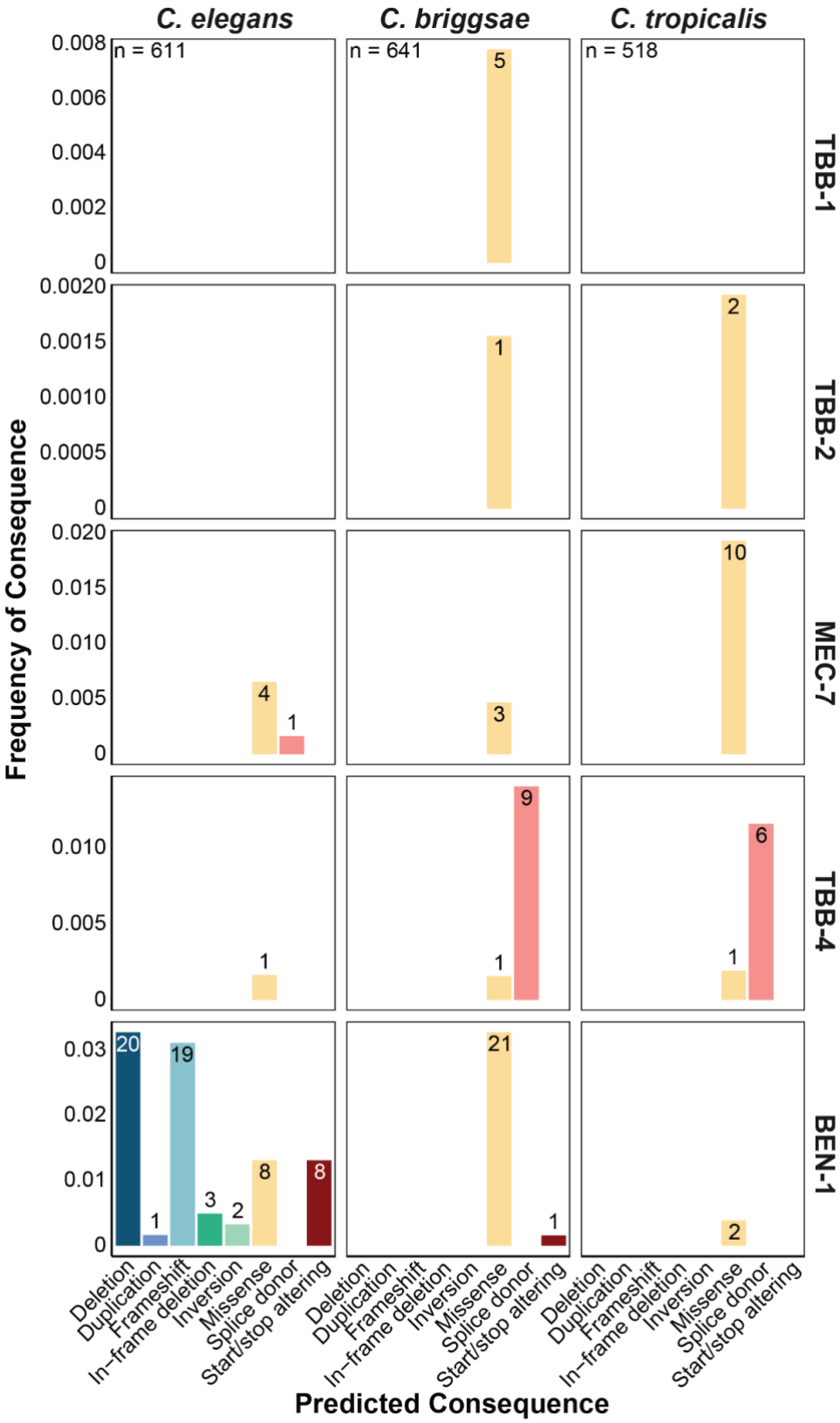

Fig 4. The frequency of predicted high-impact consequences in the five conserved beta-tubulin genes present in natural populations of *C. elegans*, *C. briggsae*, and *C. tropicalis*.
The frequency of single nucleotide variants (SNVs) and structural variants (SVs) present in natural populations of *C. elegans* (n = 611), *C. briggsae* (n = 641), and *C. tropicalis* (n = 518) (y-axis) are shown by their predicted

consequence in each beta-tubulin gene (x-axis). The total number of isotype reference strains with a given predicted consequence are displayed on top of each bar plot.

Differences in tissue- and cell-specific expression patterns of beta-tubulins might influence BZ susceptibility

Tissue-specific differences in beta-tubulin expression among the three *Caenorhabditis* species could influence BZ resistance. To compare beta-tubulin expression patterns, we analyzed two whole-animal single-cell transcriptomic datasets that quantify gene expression patterns across *C. elegans*, *C. briggsae*, and *C. tropicalis* [42,43]. A comparison of embryonic gene expression levels in *C. elegans* and *C. briggsae* revealed that beta-tubulin gene expression during embryogenesis is highly conserved (**S9 Table and S10 Table**). On average, the five beta-tubulin gene distances, which quantify expression conservation across homologous cell-types, were small (mean beta-tubulin JSDgene = 0.29), which indicated conserved embryonic expression patterns between *C. elegans* and *C. briggsae* (JSDgene < 0.45) (**S9 Table**) [43]. Expression breadth across cell-types (*i.e.*, cell-type specificity) was also conserved. The broad expression of *tbb-1* and *tbb-2*, and the cell-specific expression of *ben-1*, *tbb-4*, and *mec-7* are conserved between *C. elegans* and *C. briggsae* during embryogenesis (**S10 Table**). Among beta-tubulin genes, *tbb-2* displayed the greatest divergence in embryonic gene expression breadth, the largest difference across species in cell-type specificity (**S10 Table**). Overall, embryonic beta-tubulin expression patterns are conserved between *C. elegans* and *C. briggsae*, although *tbb-2* expression breadth is an exception (**S10 Table**). Next, because neuronal *ben-1* expression restores BZ susceptibility in *C. elegans* [33]we focused on the divergence of beta-tubulin expression across homologous neuronal cell classes at the L2 larval stage [43]. For each gene, we quantified neuron-class-specific expression divergence across the three *Caenorhabditis* species using the proportion of neuronal classes where gene expression differs among species (**S11 Table**) [43]. At least one species expressed *ben-1* in 98 of 118 neuronal cell classes. However, all three *Caenorhabditis* species expressed *ben-1* in only 35 of these classes (Jaccard distance = 0.64) (**S11 Table**). By contrast, *tbb-1* and *tbb-2* had highly conserved expression across the three *Caenorhabditis* species (98 of 118 neuronal cell classes expressed *tbb-1* or *tbb-2* in all three species) (Jaccard distance = 0) (**S11 Table**) [43]. The broad and conserved neuronal expression of *tbb-1* and *tbb-2* contrasts with *ben-1*, which showed narrower and species-specific expression patterns. Next, because *ben-1* expression in

373 cholinergic neurons restores BZ susceptibility in *C. elegans [33]*, we compared cholinergic neuronal expression
374 and identified several cell classes with species-specific patterns. Generally, beta-tubulin cell-specificity is
375 conserved across the three *Caenorhabditis* species (**S9 Table**, **S10 Table**, **S11 Table**). However, examples of
376 expression divergence among *C. elegans*, *C. briggsae*, and *C. tropicalis* were identified for *ben-1* and *tbb-2.* The
377 divergence in *ben-1* expression across cholinergic cell classes indicates that the neuronal sites where *ben-1*
378 function causes BZ susceptibility could differ among species. Future work should test this hypothesis using
379 transgenic strains that express *ben-1* in different tissues and neuronal cells.

380 **The most diverse high-impact variants are found in *Cel-ben-1***

381 To better understand the evolution of predicted BZ resistance alleles in the three *Caenorhabditis* species,
382 we assessed the population-wide frequencies of each beta-tubulin variant. First, to determine the prevalence of
383 high-impact variants in the five conserved beta-tubulin genes (*tbb-1*, *tbb-2*, *mec-7*, *tbb-4*, and *ben-1*) across
384 *Caenorhabditis* species, we quantified the frequency of each variant (deletion, duplication, frameshift, in-frame
385 deletion, inversion, missense, splice donor, and start/stop altering) in each species. With global sampling of the
386 three *Caenorhabditis* species (*C. elegans*: 611 strains, *C. briggsae*: 641 strains, *C. tropicalis*: 518 strains), we
387 found that *C. elegans* variants predicted to cause deleterious functional effects were present in 1% of strains. By
388 contrast, variants predicted to cause deleterious functional effects in *C. briggsae* and *C. tropicalis* were rare (<
389 0.05% of all strains in either species) (**Fig. 4**). The most variation in beta-tubulin genes was identified in *Cel-ben-*
390 *1*, where deletions, frameshifts, in-frame deletions, inversions, missense, stop/start altering variants, and a
391 duplication were found. Next, we found one missense variant in *Cel-tbb-4* and several missense variants and a
392 splice donor in *Cel-mec-7*. Overall, *C. elegans* has acquired the most diverse set of high-impact variants in and
393 predicted functional effects on *ben-1*. In *C. briggsae*, we found 21 missense amino acid substitutions and a single
394 start/stop altering consequence in *Cbr-ben-1*. In both *Cbr-tbb-1* and *Cbr-tbb-2*, we identified rare missense
395 consequences. Additionally, we found nine strains with splice variants in *Cbr-tbb-4* and one strain with a
396 missense variant. In *C. tropicalis*, we found missense consequences in all beta-tubulin genes, except *tbb-1*.
397 Additionally, we found six strains with splice variants in *Ctr-tbb-4*. These findings highlight that *Cel-ben-1* has the
398 most diverse set of variants, reinforcing its role in BZ resistance.

399 Next, we examined the geographic distribution of strains carrying high-impact variants in *tbb-1*, *tbb-2*,

400 *mec-7*, *tbb-4*, and *ben-1* to determine if beta-tubulin variants were associated with natural sampling location. In
401 *C. elegans*, variants in *ben-1* were found globally with no discernible geographic pattern but were concentrated
402 in clades that have experienced recent selective sweeps [44,45] (**Fig. 5**). *Cel-ben-1* variants in swept clades
403 suggest that these mutations arose as relatively recent evolutionary events in response to BZ-like compounds
404 in the natural niche. By contrast, in *C. briggsae*, variants in *ben-1* were distributed throughout the species tree
405 and found on more ancestral branches (*i.e.*, earlier diverged lineages in the species) (**Fig. 5C**). For *C. tropicalis*,
406 the limited number of variants in *ben-1* precludes any definitive conclusions regarding their evolutionary patterns
407 (**Fig. 5D**). Because few variants are found in *tbb-1* (**S26 Fig.**), *tbb-2* (**S27 Fig.**), *mec-7* (**S28 Fig.**), and *tbb-4* (**S29**
408 **Fig.**), we cannot identify the evolutionary patterns of BZ resistance in these genes for any of the three species.

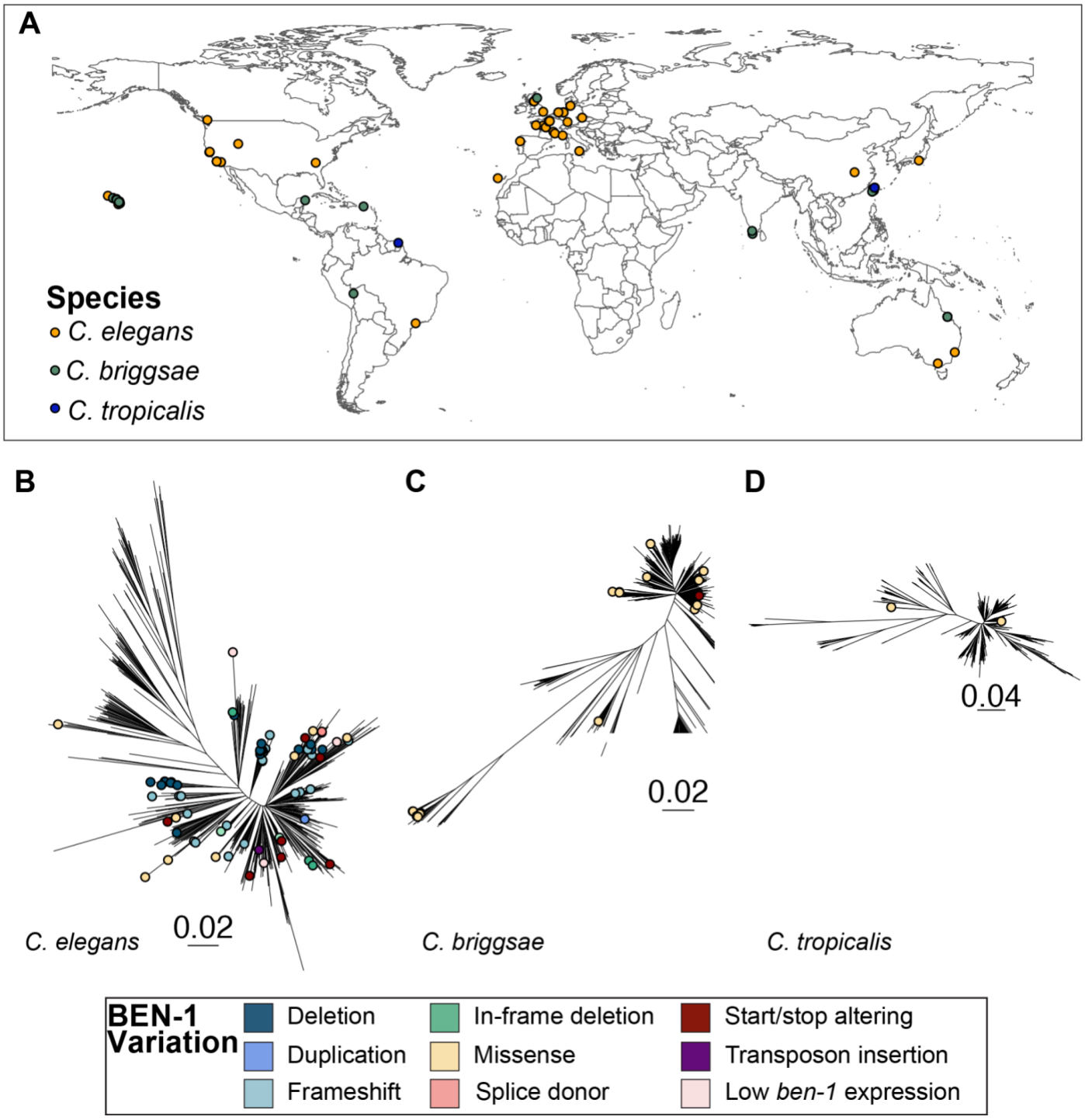

Fig 5. The global distribution of *Caenorhabditis* strains that contain predicted high-impact variation in BEN-1.
(A) Each point corresponds to the sampling location of an individual *C. elegans* (orange), *C. briggsae* (green), or *C. tropicalis* (blue) isotype reference strain with a predicted high-impact consequence in BEN-1. A genome-wide phylogeny of **(B)** 611 *C. elegans*, **(C)** 641 *C. briggsae*, and **(D)** 518 *C. tropicalis* isotype reference strains, where each point denotes an isotype reference strain with a predicted high-impact consequence in BEN-1 is shown.

Finally, because substrates harbor distinct microbial communities that can influence the evolution of BZ

420 resistance alleles, we determined if strains carrying a high-impact variant in a beta-tubulin gene were associated
421 with specific substrates. We performed substrate enrichment analysis to assess correlations between 12
422 substrates and all strains in the three *Caenorhabditis* species (**S12 Table**). However, no significant enrichment
423 was observed between a high-impact variant in a beta-tubulin gene and any given substrate (Fisher's Exact
424 Test, p=1) (**S30 Fig.**). Because no geographic or substrate enrichment was observed, evolutionary pressures
425 driving beta-tubulin variation are likely not strongly tied to substrate.
426

427 **DISCUSSION**

428 **Beta-tubulin-mediated BZ resistance varies across natural populations of *Caenorhabditis* nematodes**

429 This study provides new insights into beta-tubulin-mediated ABZ resistance across three *Caenorhabditis*
430 species. Each *Caenorhabditis* species harbored a unique set of predicted high-impact beta-tubulin alleles, but
431 only variants in *ben-1* conferred resistance. With additional wild strains since our first study, we identified
432 additional *Cel-ben-1* LoF alleles associated with BZ resistance, which confirmed that a diverse collection of
433 predicted LoF variants in *ben-1* are associated with ABZ resistance in *C. elegans* [14,16]. In *C. briggsae*, strains
434 harboring only two of the eight unique *Cbr-ben-1* variants were resistant to ABZ. One *Cbr-ben-1* variant
435 (W21stop) causes early protein termination, and the other (Q134H) alters a residue within the *Cbr*-BEN-1 protein
436 that likely affects ABZ binding and is associated with resistance in *A. caninum [11]*. A CRISPR-Cas9-generated
437 deletion of *Cbr-ben-1* conferred resistance similar to that displayed by wild strains with these alleles and did not
438 impact fitness. To date, resistance has yet to be identified in *C. tropicalis* wild strains. However, a CRISPR-Cas9-
439 generated deletion of *Ctr-ben-1* conferred resistance and caused a significant reduction in fitness (fecundity),
440 which likely explains why just two high-impact variants were identified among wild strains and neither caused
441 loss of *ben-1* function. Overall, our results highlight the complexity of BZ resistance. Accurate prediction of BZ
442 resistance across nematode species requires a clear understanding of the contributions of both beta-tubulin
443 dependent and beta-tubulin independent mechanisms.
444

445 **Nematode survival under BZ exposure depends on beta-tubulin dosage and drug-binding ability**

446 BZs bind to beta-tubulins and inhibit the polymerization of microtubules [2–4]. Therefore, despite the

447 presence of beta-tubulin independent resistance mechanisms [46,47], beta-tubulins have a large impact on BZ
448 efficacy as an anthelmintic treatment. Two factors determine how beta-tubulin impacts susceptibility to BZs: (1)
449 the beta-tubulin's ability to bind to BZs and (2) the dosage of the beta-tubulin protein, which can be modified by
450 tissue-specific expression. Nematode species have distinct beta-tubulin gene complements with divergence in
451 number of genes, BZ binding affinities, expression levels and cell types, and redundancy. Ultimately, this
452 divergence in beta-tubulin complement shapes the type(s) of resistance-associated alleles that arise in each
453 nematode species. In species where the primary BZ-binding beta-tubulin is redundant with other isoforms, as in
454 selfing *Caenorhabditis* species, loss of a single copy can confer resistance without disrupting essential
455 microtubule functions. In species without redundancy, such as *H. contortus*, beta-tubulin variants that alter the
456 BZ binding affinity are the only available beta-tubulin dependent route to BZ resistance.

457 In *C. elegans*, *ben-1* is the primary target of BZs but is redundant with *tbb-1* and *tbb-2* [28–30]. LoF alleles
458 in *ben-1* reduce the total amount of BZ-binding protein while preserving essential microtubule functions, which
459 permits nematode development during BZ exposure. A similar pattern likely occurs in *C. briggsae*, where rare
460 high-impact variants in *ben-1* confer resistance, and other beta-tubulin genes maintain essential microtubule
461 functions. By contrast, *H. contortus* relies on the essential beta-tubulin *tbb-isotype-1* and cannot tolerate loss
462 without severe fitness consequences [18]. The differences between the *Caenorhabditis* species and *H. contortus*
463 demonstrate that the prediction of beta-tubulin dependent resistance requires the identification of the total
464 number and expression levels of beta-tubulin genes and determination of which encoded beta-tubulins can bind
465 to BZ. Altogether, BZ resistance depends not on the copy number of beta-tubulins alone but on the availability
466 of functional beta-tubulins capable of interacting with BZs.

467

468 **How can we accurately predict BZ resistance across nematode species?**

469 To accurately predict BZ resistance across nematode species, we need (1) tractable nematode models
470 with beta-tubulin gene complements that resemble that of parasite species, (2) improved parasitic nematode
471 genomes that enable the comprehensive identification of beta-tubulin genes, (3) functional tests that define how
472 parasite beta-tubulin alleles contribute to BZ response, and (4) to define the contribution of non-beta-tubulin
473 genes to overall BZ response. To date, no experimentally tractable model nematode species exist with beta-

474 tubulin genes that have both limited redundancy and BZ binding properties similar to those of parasitic
475 nematodes. *Pristionchus pacificus*, a free-living clade V nematode has three beta-tubulin genes, comprising two
476 *ben-1* orthologs (*Ppa-ben-1.1* and *Ppa-ben-1.2*) and an ortholog of *Cel-mec-7* (*Ppa-mec-7*) [48]. All three beta-
477 tubulin genes in *Pristionchus pacificus* are predicted to have high ABZ binding affinity (**S31 Fig.**). Using CRISPR-
478 Cas9 genome editing, we found that homozygous LoF alleles for either *Ppa-ben-1.1* or *Ppa-ben-1.2* could not
479 be recovered in *P. pacificus*, suggesting that both genes are essential **(S13 Table**). The fact that *P. pacificus*
480 has fewer beta-tubulin genes than *C. elegans* likely contributes to the lack of redundancy among beta-tubulins.
481 The number, essentiality, and BZ binding affinity of the *P. pacificus* beta-tubulins more closely resembles that of
482 *H. contortus*, which positions *P. pacificus* as a valuable free-living model to study essential beta-tubulin function,
483 beta-tubulin dosage effects, and BZ resistance relevant to parasitic nematode species.

484 Second, to understand the role beta-tubulins play in BZ resistance across parasitic nematode species,
485 we must significantly improve genomes and gene models. Most parasitic nematode genomes remain incomplete
486 or are poorly annotated, which obscures beta-tubulin copy number and gene identity. Recent efforts have
487 produced higher quality genomes for some parasitic nematodes [49–51], but we must still define beta-tubulin
488 copy number across diverse nematode species. For example, improved reference genomes and gene models
489 for *C. briggsae* [52,53] and *C. tropicalis* [54] enabled accurate beta-tubulin gene identification for these species.
490 Until genome assemblies, technologies, and analytical techniques improve, we will be unable to accurately
491 predict the number of beta-tubulin genes in a given species and their respective BZ binding affinities.

492 Third, functional validation of parasitic resistance alleles presents additional challenges. Although tools
493 such as RNAi can work in parasitic nematodes [55], delivery challenges and difficulty isolating edited individuals
494 limit its use. An alternative strategy is to introduce predicted parasite resistance alleles into *C. elegans* to test
495 effects on fitness and BZ response, as shown previously [14–16]. Finally, some parasitic nematodes, such as
496 ascarid species, exhibit BZ resistance without known beta-tubulin resistance alleles [56–58]. This pattern
497 suggests that resistance arises independently of detected beta-tubulin sequence changes or reflects incomplete
498 identification of beta-tubulin genes caused by poor genome assemblies. To date, the underlying cause of BZ
499 resistance in ascarid species remains unclear. Reduced functional beta-tubulin dosage, altered BZ binding, or
500 both could contribute to BZ resistance in ascarids [59]. Improved genome assemblies and annotation are

501 required to identify all beta-tubulin genes and drug-binding sites to define the mechanisms of BZ resistance in
502 ascarid species. In the future, the introduction of newly identified ascarid alleles into free-living nematode models
503 can directly test resistance and fitness, and clarify the mechanisms that drive BZ resistance in clade III
504 nematodes. Additionally, we must define how redundancy, essentiality, beta-tubulin dosage, and drug-binding
505 properties shape the evolution of resistance to improve the prediction of BZ resistance across the huge diversity
506 of parasitic nematode species.

507 **MATERIALS AND METHODS**

508 **Identification of beta-tubulin loci**

509 Amino acid sequences for all six *C. elegans* beta-tubulin proteins were obtained from WormBase
510 (WS283) [60] and used as queries in a BLASTp search (Version 2.12.0) [61] against protein sequence databases
511 constructed using gene models for *C. briggsae* [53] and *C. tropicalis* [62]. To construct the protein sequence
512 database, we extracted gene model transcript features from the gene feature file with *gffread* (Version 0.9.11)
513 [63] and processed them using the *makeblastdb* function from BLAST (Version 2.12.0). From the BLASTp
514 search, we identified *C. briggsae* and *C. tropicalis* protein sequences with the highest percent identity (PID) to
515 each *C. elegans* beta-tubulin protein. Only protein sequences with the highest PID in both searches were
516 considered orthologs (**S14 Table**). For some *C. elegans* beta-tubulin orthologs, multiple *C. briggsae* or
517 *C. tropicalis* gene models contained multiple splice isoforms. All gene models for all beta-tubulin transcripts were
518 manually inspected, and isoforms that were not fully supported by short-read RNA sequencing data were
519 removed.
520

521 **Single nucleotide variant (SNV) and indel calling and annotation**

522 To identify single nucleotide variants (SNVs) or indels (insertions and deletions) in the beta-tubulin genes
523 across the selfing *Caenorhabditis* species, we used the Variant Annotation Tool from the *Caenorhabditis* Natural
524 Diversity Resource (CaeNDR) (Release IDs: *C. elegans* - 20231213, *C. briggsae* - 20240129, *C. tropicalis* -
525 20231201) [36]. The identified SNVs and indels included small insertions and deletions, frameshifts, altered stop
526 and start codons, nonsynonymous changes, and splice variants (**S1 Table, S2 Table, and S3 Table**).

527

528 **Structural variant (SV) calling and annotation**

529 Structural variant (SV) calling was performed using *DELLY* (Version 0.8.3), a SV caller optimized to detect
530 large insertions, deletions, and other complex structural variants such as inversions, translocations, and
531 duplications in paired-end short-read alignments [64] and shown to perform well on *C. elegans* short-read
532 sequence data [65]. SVs that overlapped with beta-tubulin genes were extracted using *bcftools* (Version 1.10.1)
533 [66]. Insertions, deletions, inversions, and duplications that passed the *DELLY* (Version 0.8.3) default quality
534 threshold (greater than three supporting read pairs with a median MAPQ > 20), filtered to high-quality genotypes
535 (genotype quality > 15), and had at least one alternative allele were retained. For complex variants (inversions
536 and duplications), the identification of at least one split-read pair was required (variants flagged as a precise SV
537 by *DELLY*). To validate SVs that passed quality filtering, each SV was manually inspected for breakpoints in the
538 raw-read alignments (*Wally*, Version 0.5.8) and for impacts on the beta-tubulin coding sequence (CaeNDR
539 Genome Browser) [36] (**S15 Table**). We retained SVs where raw read alignments suggested that the SV
540 impacted the beta-tubulin coding sequence. We compared the *Cel-ben-1* SVs called by *DELLY* to those SVs
541 identified previously [14]. *DELLY* successfully recalled structural variants in several strains, including deletions
542 in JU751, JU830, JU1395, JU2582, JU2587, JU2593, JU2829, and QX1233, as well as an inversion in MY518.
543 However, *DELLY* did not detect a previously reported transposon insertion in strain JU3125. To assess if other
544 SVs could have been missed by *DELLY*, we manually inspected the read alignments for all strains that had not
545 been previously phenotyped to check if any other SVs were not detected by *DELLY*. We confirmed the presence
546 of novel *Cel-ben-1* SVs in multiple strains, including putative deletions in ECA706 and NIC1832, and a duplication
547 in NIC1107. Additionally, we identified a previously undetected putative deletion in JU4287. We also examined
548 the amino acids at position 200 in TBB-1, TBB-2, MEC-7, TBB-4, and BEN-1 orthologs and found that all MEC-
549 7, TBB-4, and BEN-1 orthologs contained phenylalanine, and that all TBB-1 and TBB-2 orthologs contained
550 tyrosine at position 200 (**S31 Fig.**).

551

552 **Association of *Cel-ben-1* expression with ABZ response**

553 Two previous assays measured developmental responses of wild *C. elegans* strains after ABZ exposure
554 [14,67]. For 180 of these wild *C. elegans* strains, whole-animal expression levels (transcripts per million
555 estimates [TPM]) were collected from untreated young-adult animals [38]. We identified strains with low *Cel-ben-*
556 *1* expression by selecting strains with TPM values more than one standard deviation (SD) below the mean
557 expression level across all 207 wild strains with expression data. Of the 180 wild *C. elegans* strains, 105 strains
558 were measured for both ABZ response and gene expression. A linear model was built using the *lm* function in R
559 to account for assay effects. Subsequently, the residuals of the linear model were used to normalize previous
560 measures of ABZ response. We evaluated the linear fit between each strain's expression of *ben-1* (**S1 Fig.**), *tbb-*
561 *1*, *tbb-2*, *mec-7*, or *tbb-4* (**S19 Fig.**) and the developmental delay following ABZ exposure.
562

563 **Phylogenetic analysis**

564 We characterized the relatedness of isotype reference strains (genetically unique strains) with beta-
565 tubulin variants using species trees downloaded from CaeNDR and generated by the 'post-gatk-nf' pipeline
566 (https://github.com/AndersenLab/post-gatk-nf) (Release IDs: *C. elegans* - 20231213, *C. briggsae* - 20240129,
567 *C. tropicalis* - 20231201) [36]. Briefly, the trees were generated using high-quality SNVs in isotype reference
568 strains retained in the hard-filtered variant call format (VCF) file. *vcf2phylip* [68] and the *bioconvert* [69] function
569 *phylip2stockholm* were used to prepare inputs for *quicktree*, which was used to construct a tree using a neighbor-
570 joining algorithm [70]. All versions of these software can be accessed from the 'post-gatk' docker container
571 (https://hub.docker.com/r/andersenlab/tree), used by the 'post-gatk-nf' pipeline. We visualized the trees for each
572 species using the *ggtree* function from the *ggtree* (v3.6.2) R package [71].
573

574 **Strain selection and maintenance**

575 Eighteen *C. elegans* strains, 45 *C. briggsae* strains, and 15 *C. tropicalis* strains from the CaeNDR [36]
576 were used in this study (**S1 Table, S2 Table, and S3 Table)**. Isolation details for each strain are included in
577 CaeNDR. For each species, we selected strains that had variants (SNV or SV) with unique high-impact
578 consequences in *tbb-1*, *tbb-2*, *mec-7*, *tbb-4*, or *ben-1* that had not been previously phenotyped. High-impact
579 consequences included changes to amino acids, start and stop codon positions, or splice variants [36]. Strains

580 with high-impact consequences in a beta-tubulin gene are herein referred to as “predicted resistant” strains.
581 Strains that were closely related to predicted resistant strains with no high-impact consequences in beta-tubulin
582 genes were also included for *C. briggsae* and *C. tropicalis* and herein classified as “predicted susceptible” strains
583 (**S2 Fig., S3 Fig., and S4 Table**). The reference strains for all three species were included.

584 Before measuring ABZ responses, *C. elegans* and *C. briggsae* animals were maintained at 20ºC and
585 *C. tropicalis* animals were maintained at 25ºC. All animals were maintained on 6 cm plates with modified
586 nematode growth medium (NGMA), which contains 1% agar and 0.7% agarose to prevent animals from
587 burrowing [72]. The NGMA plates were seeded with the *Escherichia coli* strain OP50 as a nematode food source.
588 All strains were grown for three generations without starvation on NGMA plates before anthelmintic exposure to
589 reduce the transgenerational effects of starvation stress [73].

590

591 **CRISPR-Cas9 genome editing**

592 To validate the role that *ben-1* plays in ABZ resistance in the three *Caenorhabditis* species, we used
593 CRISPR-Cas9 to create *ben-1* deletions. For *C. elegans*, we used a previously generated strain (ECA882) with
594 a *ben-1* deletion in the N2 background [14,15,27,37]. The *ben-1* deletions were generated in the AF16
595 background for *C. briggsae* and the NIC58 background for *C. tropicalis*. Injections were performed by InVivo
596 Biosystems (Eugene, OR), and deletions of *Cbr-ben-1* and *Ctr-ben-1* were confirmed using PCR (**S10 Fig. and**
597 **S11 Fig.**). Briefly, two primer pairs were designed for the deletion alleles for each species, with each pair
598 designed to bind to a region external or internal to both of the deletions. Confirmation of deletion was performed
599 by performing two amplification reactions for each sample: (1) the use of both external primers, and (2) the use
600 of an internal and external pair (**S5 Table**). The parental strain was used as a control in each PCR. Deletions
601 were confirmed by a reduction in the size of the external-external amplicon in the edited strains compared to the
602 unedited parental control strain. Homozygosity was confirmed by the loss of a band amplified from the external-
603 internal primer pair. Edited strains underwent two generations of PCR confirmation for homozygosity. Two
604 independent edits of each allele in each species were generated to control for any potential off-target effects
605 caused by CRISPR-Cas9 genome editing (**S12 Fig., S13 Fig., and S5 Table**).

606

607 **Nematode food preparation for NGMA 6 cm plates**

608 The OP50 *E. coli* strain was used as a nematode food source for NGMA plates. A frozen stock of OP50
609 was streaked onto a 10 cm Luria-Bertani (LB) agar plate and incubated overnight at 37ºC. The following day, a
610 single bacterial colony was transferred into each of two culture tubes that contained 5 mL of 1x LB. The starter
611 cultures and two negative controls (1X LB without *E. coli*) were incubated for 18 hours at 37ºC shaking at 210
612 rpm. The OD_{600} value of the starter cultures were measured using a spectrophotometer (BioRad, SmartSpec
613 Plus) to calculate how much starter culture was needed to inoculate a 1 L culture at an OD_{600} value of 0.005. For
614 each assay, one culture containing 1 L of pre-warmed 1X LB inoculated with the starter culture grew for
615 approximately 4 - 4.5 hours at 37ºC at 210 rpm to an OD_{600} value between 0.45 and 0.6. Cultures were
616 transferred to 4ºC to slow growth. OP50 was spotted on NGMA test plates (two per culture) and grown at 37ºC
617 overnight to assay for contamination.

618

619 **Nematode food preparation for high-throughput larval development assays (HTLDAs)**

620 One batch of HB101 *E. coli* was used as a nematode food source for all HTLDAs in this study. A frozen
621 stock of HB101 *E. coli* was streaked onto a 10 cm LB agar plate and incubated overnight at 37ºC. The following
622 day, a single bacterial colony was transferred into three culture tubes that contained 5 mL of 1x Horvitz Super
623 Broth (HSB). The starter cultures and two negative controls (1X HSB without *E. coli*) were incubated for 18 hours
624 at 37ºC shaking at 180 rpm. The OD_{600} value of the starter cultures were measured using a spectrophotometer
625 (BioRad, SmartSpec Plus) to calculate how much starter culture was needed to inoculate a 1 L culture at an
626 OD_{600} value of 0.001. A total of four cultures each containing 1 L of pre-warmed 1X HSB inoculated with the
627 starter culture grew for 15 hours at 37ºC while shaking at 180 rpm. After 15 hours, flasks were removed from the
628 incubator and transferred to 4ºC to slow growth. The 1X HSB was removed from the cultures by performing three
629 rounds of centrifugation, where the supernatant was removed, and the bacterial cells were pelleted. Bacterial
630 cells were washed with K medium, resuspended in K medium, pooled, and transferred to a 2 L glass beaker.
631 The OD_{600} value of the bacterial suspension was measured and diluted to a final concentration of OD_{600}100 with
632 K medium, aliquoted to 15 mL conicals, and stored at -80ºC for use in the HTLDAs.

633

634 **ABZ dose-response assays for *C. briggsae* and *C. tropicalis***

635 Because ABZ response had been minimally characterized in *C. briggsae* [74] and has not yet been
636 described in *C. tropicalis*, we first measured dose-response curves for both species after exposure to ABZ to
637 assess developmental delay. Before performing HTLDAs, ABZ (Sigma-Aldrich, Catalog # A4673-10G) stock
638 solutions were prepared in dimethyl sulfoxide (DMSO) (Fisher Scientific, Catalog # D1281), aliquoted, and stored
639 at -20ºC for use in the assays. For the dose-response assays, animals were exposed to ABZ at the following
640 concentrations (µM): 0 (1% DMSO), 0.12, 0.23, 0.47, 0.94, 1.88, 3.75, 7.5, 15, 30, 60, and 120. Animals
641 developed in the presence of ABZ as described in *HTLDAs to assess nematode development*.

642 Dose-response model estimation and statistics were performed as described previously [67,75]. Briefly,
643 a four-parameter log-logistic dose-response curve was fit independently for a genetically diverse set of 11 *C.*
644 *briggsae* strains (**S14 Fig.**) and seven *C. tropicalis* strains (**S16 Fig.**), where normalized median animal length
645 was used as a metric for phenotypic response (see *HTLDA data collection and data cleaning*). For each strain-
646 specific dose-response model, slope (*b*) and concentration (*e*) were estimated with strain as a covariate. We
647 calculated EC_{10} as we have previously found EC_{10} response to be more heritable than half maximal effective
648 concentration (EC_{50}) estimates and were used in our analysis [67,75]. A dosage of 30 µM ABZ was closest to
649 the EC_{10} for *C. briggsae* and *C. tropicalis*, consistent with ABZ concentrations used in past *C. elegans* assays
650 [15,16,37] and in all HTLDAs in this study.

651

652 **HTLDAs to assess nematode development**

653 Populations of each strain were amplified and bleach-synchronized in three independent assays.
654 Independent bleach synchronizations controlled for variation in embryo survival and subsequent effects on
655 developmental rates. After bleach synchronization, approximately 30 embryos were dispensed into each well of
656 a 96-well microplate in 50 µL of K medium. Each strain had sixteen wells per condition (DMSO or ABZ) in each
657 assay. Three independent assays yielded a total of forty-eight wells per condition per strain. Each 96-well
658 microplate was prepared, labeled, and sealed using gas-permeable sealing films (Fisher Scientific, Catalog #
659 14-222-043). Plates were placed in humidity chambers to incubate for 24 hours at 20°C for *C. elegans* and
660 *C. briggsae*, and 25°C for *C. tropicalis* while shaking at 170 rpm (INFORS HT Multitron shaker). After 24 hours,

661 every plate was inspected to ensure that all embryos hatched and animals were developmentally arrested at the
662 first larval (L1) stage so all strains started each assay at the same developmental stage. Next, food was prepared
663 to feed the developmentally arrested L1 animals using the required number of OD_{600}100 HB101 aliquots (see
664 *Nematode food preparation for HTLDAs*). The HB101 aliquots were thawed at room temperature, combined into
665 a single conical tube, and diluted to an OD_{600}30 with K medium. To inhibit further bacterial growth and prevent
666 contamination, 150 µL of kanamycin was added to the HB101. An aliquot of 100 µM ABZ stock solution was
667 thawed at room temperature and added to an aliquot of OD_{600}30 K medium at a 3% volume/volume ratio. Next,
668 25 µL of the food and ABZ mixture was transferred into the appropriate wells of the 96-well microplates to feed
669 the arrested L1 animals at a final HB101 concentration of OD_{600}10 and expose L1 animals to ABZ. Immediately
670 afterward, the 96-well microplates were sealed using a new gas permeable sealing film, returned to the humidity
671 chambers, and incubated for 48 hours at 20°C (*C. elegans* and *C. briggsae*) or 42 hours at 25°C (*C. tropicalis*)
672 while shaking at 170 rpm. After 48 hours (*C. elegans* and *C. briggsae*) or 42 hours (*C. tropicalis*) of incubation
673 and shaking in the presence of food and either DMSO or ABZ, the 96-well microplates were removed from the
674 incubator and treated with 50 mM sodium azide in M9 for 10 minutes to paralyze and straighten nematodes.
675 After 10 minutes, images of nematodes in the microplates were immediately captured using Molecular Devices
676 ImageXpress Nano microscope (Molecular Devices, San Jose, CA) using a 2X objective. The ImageXpress
677 Nano microscope acquires brightfield images using a 4.7 megapixel CMOS camera and stores images in a 16-
678 bit TIFF format. The images were used to quantify the development of nematodes in the presence of DMSO or
679 ABZ as described below (see *High-throughputput imager assays [HTLDA] data collection and cleaning*). A full
680 step-by-step protocol for the HTLDA has been deposited on protocols.io [76].
681

682 **HTLDA data collection and data cleaning**

683 *CellProfiler* (Version 24.10.1) was used to characterize and quantify biological data from the image-based
684 assays. Custom software packages designed to extract animal measurements from images collected on the
685 Molecular Devices ImageXpress Nano microscope were previously described [77]. *CellProfiler* modules and
686 *WormToolbox* were developed to extract morphological features of individual animals from images from the
687 HTLDA [78]. Worm model estimations and custom *CellProfiler* pipelines were written using the *WormToolbox* in

688 the GUI-based instance of *CellProfiler* [75]. Next, a Nextflow pipeline (Version 24) was written to run command-
689 line instances of *CellProfiler* in parallel on the Rockfish High-Performance Computing Cluster (Johns Hopkins
690 University). The *CellProfiler* workflow can be found at https://github.com/AndersenLab/cellprofiler-nf. The custom
691 *CellProfiler* pipeline generates animal measurements by using four worm models: three worm models tailored to
692 capture animals at the L4 larval stage, in the L2 and L3 larval stages, and the L1 larval stage, as well as a "multi-
693 drug high dose" (MDHD) model, to capture animals with more abnormal body sizes caused by extreme
694 anthelmintic responses. These measurements comprised our raw dataset. Two *C. briggsae* strains (NIC1052
695 and VX34) were not fully paralyzed and straightened at the time of imaging, which created some misclassification
696 of animal measurements. Thus, the animal lengths for strains NIC1052 and VX34 measured by *CellProfiler* are
697 shorter than the actual animal lengths. However, the difference in animal lengths does not affect the classification
698 of a strain as resistant or sensitive to ABZ. Data cleaning and analysis steps were performed using a custom R
699 package, *easyXpress* (Version 2.0) [77] and followed methods previously reported [37]. All analyses were
700 performed using the R statistical environment (Version 4.2.1) unless stated otherwise.
701

702 ***C. briggsae* and *C. tropicalis* fecundity assays**

703 To define the fitness costs associated with a loss of *ben-1* in *C. briggsae* and *C. tropicalis*, we performed
704 fecundity assays. For *C. briggsae*, we used the two strains with independent edits of *ben-1* in the AF16
705 background (ECA3953 and ECA3954) and the AF16 reference strain. For *C. tropicalis*, we used the two strains
706 with independent edits of *ben-1* in the NIC58 background (ECA4247 and ECA4248) and the NIC58 reference
707 strain. To perform fecundity assays, we placed a single L4 larval stage hermaphrodite from each strain onto a 6
708 cm NGMA plate that was spotted with *E. coli* OP50. *C. briggsae* assay plates were maintained at 20°C, and
709 *C. tropicalis* assay plates were maintained at 25°C. For each assay plate, the original hermaphrodite parent was
710 transferred to a fresh 6 cm NGMA plate every 24 hours for 192 hours. Ten technical replicates were prepared
711 for each strain. The Basic Imaging Platform from Tau Scientific was used to collect images for each of the assay
712 plates (0, 24, 48, 72, 96, and 120-hours) at either 48 or 72 hours for *C. briggsae* and *C. tropicalis* animals,
713 respectively, after the removal of the parent from each NGMA plate. The total offspring was counted from each
714 image by visual inspection using the Multi-point tool in ImageJ (Version 1.54g). The original hermaphrodite

715 parents were excluded from the counts. Replicates where the original hermaphrodite parent died were excluded
716 from the analysis. Only biological replicates with data from at least six assay plates were used to calculate total
717 fecundity (**S15 Fig., S6 Table, and S7 Table**).
718

719 **Tissue-specific beta-tubulin gene expression conservation in *C. elegans*, *C. briggsae*, and *C. tropicalis***

720 To assess beta-tubulin expression divergence across neuronal cell classes, we used whole-animal
721 single-cell transcriptomes of *C. elegans*, *C. briggsae*, and *C. tropicalis* [43]. We quantified neuronal cell
722 expression divergence across species using precomputed Jaccard distances calculated from the neuronal cell
723 classes in at least one species and the number of neuron classes in which a gene is expressed in all three
724 species [43]. We also downloaded gene expression summary data for each homologous cell class from
725 *CaenoGen* and analyzed expression patterns in cell classes that used acetylcholine (ACh) as a neurotransmitter
726 in *C. elegans [79]*. We identified cell classes in which *ben-1* orthologs showed species-specific presence or
727 absence of expression.

728 We also analyzed embryonic single-cell transcriptomes from the *C. briggsae* and *C. elegans* reference
729 strains to examine the conservation of beta-tubulin gene expression in homologous cell types [42]. We used pre-
730 computed summary statistics to quantify two components of expression divergence among beta-tubulin genes:
731 gene distance (reported as Jensen-Shannon Distances for each gene) and expression breadth (reported as Tau
732 metrics for each species). Beta-tubulin gene distances and expression breadth metrics are available in the gene
733 data summary table file (**S9 Table and S10 Table**). Estimates for three cell populations are distinguished by cell-
734 type assignment: progenitor, terminal, and joint (combined progenitor and terminal cells).
735

736 **Protein structure and visualization of *ben-1* and *tbb-isotype-1* variants**

737 For *C. elegans*, the BEN-1 amino acid sequence was obtained from WormBase (WS283) [60]. For
738 *C. briggsae* and *C. tropicalis*, BEN-1 amino acid sequences were the best hits to the *C. elegans* BEN-1 query
739 from the reciprocal BLASTp search used to identify beta-tubulin orthologs (*see Identification of beta-tubulin loci*)
740 (**S16 Table**). The *H. contortus tbb-isotype-1* amino acid sequence was obtained from WormBase Parasite
741 (Version: WBPS19) [41]. Protein structures were predicted using AlphaFold3 [80]. All BEN-1 variant data and

742 associated benzimidazole-response phenotypes were compiled from this study and previously published data
743 [14,37]. A custom Python script was used to generate a PyMOL script (Version 3.1.6.1) for structural
744 visualization. Each predicted beta-tubulin structure was aligned to *Cel*-BEN-1 using the PyMOL `*align*`
745 command.
746

747 **Mutation of *ben-1* orthologs in *Pristionchus pacificus***

748 To test the function of *ben-1* in *Pristionchus pacificus*, we used CRISPR-Cas9 genome editing to delete
749 the two orthologs of *Cel-ben-1*. Designed crRNAs and tracrRNA were synthesized by Integrated DNA
750 Technologies (IDT). For the creation of the guide RNAs, 3 µL of 100 µM tracrRNA (IDT) was combined with 3
751 µL of 100 µM crRNA (IDT) and incubated at 95ºC for five minutes, followed by five minutes at room temperature
752 for annealing. The ribonucleoprotein (RNP) complex was then created by combining 0.61 µL of the guide-RNA
753 mixture with 0.25 µL of Cas9 protein (IDT), followed by incubation at 37ºC for 10 minutes. The final microinjection
754 mix was then created by combining the 0.86 µL RNP complex with 9.14 µL of a TE buffer mixture containing a
755 (55 ng/µL) plasmid containing a *P. pacificus* codon-optimized *egl-20p::TurboRFP::rpl-23UTR* construct [81] used
756 as a co-injection marker for visual identification of successful injections by the presence of fluorescent F1
757 individuals (**S13 Table)**. All F1 individuals displaying fluorescence were then isolated and allowed to self-fertilize.
758 After successful F2 embryo hatching, F1 individuals were genotyped for mutations using a heteroduplex mobility
759 assay (HMA). Individuals from F2 broods that were determined to contain heterozygous mutations in F1 mothers
760 were then isolated, allowed to self-fertilize, and genotyped by HMA after F3 embryos had hatched to identify
761 homozygous mutant lines, followed by Sanger sequencing to determine types of mutations induced. Additionally,
762 for mutations that were homozygous lethal, the F3 from heterozygous F2 individuals were likewise genotyped
763 by HMA to quantify survivability based on deviations from expected Mendelian ratios.

764 **DATA AVAILABILITY STATEMENT**

765 All code and data used to replicate the data analysis and figures are available on GitHub at:
766 https://github.com/AndersenLab/ce_cb_ct_betatubulin. S1 Table contains the list of *C. elegans* isotype reference
767 strains, any beta-tubulin variants, sample collection locations, and substrate types. S2 Table contains the list of

768 *C. briggsae* isotype reference strains, any beta-tubulin variants, sample collection locations, and substrate types.
769 S3 Table contains the list of *C. tropicalis* isotype reference strains, any beta-tubulin variants, sample collection
770 locations, and substrate types. S4 Table contains all *C. briggsae* and *C. tropicalis* isotype reference strains with
771 beta-tubulin variants and genetically related strains. S5 Table contains details about the CRISPR-Cas9 genome-
772 edited strains, CRISPR-Cas9 reagents, and oligonucleotide sequences for the deletion of *ben-1* in *C. briggsae*
773 and *C. tropicalis*. S6 Table contains the results from the fecundity assays of the *C. briggsae* reference strain
774 (AF16) and the *Cbr-ben-1* deletion strains.Table S7 contains the results from the fecundity assays of the *C.*
775 *tropicalis* strain NIC58 and the *Ctr-ben-1* deletion strains. S8 Table contains the BLOSUM62 and Granthum
776 scores for amino acid changes in the beta-tubulin genes in the three *Caenorhabditis* species. S9 Table contains
777 expression breadth (Tau) estimates for beta-tubulin genes calculated on *C. elegans* and *C. briggsae* embryonic
778 cells by Large *et al.* 2024. S10 Table contains conservation estimates of embryonic expression patterns between
779 *C. elegans* and *C. briggsae* with Jensen-Shannon gene distances estimated in Large *et al.* 2024 for beta-tubulin
780 genes. S11 Table contains the neuronal cell-class expression divergence of beta-tubulin orthologs across *C.*
781 *elegans*, *C. briggsae*, and *C. tropicalis*, reported as Jaccard distances obtained from Toker *et al.* 2025. S12
782 Table contains results from the substrate enrichment analysis. S13 Table contains details about the CRISPR-
783 Cas9 genome edited strains, CRISPR-Cas9 reagents, and oligonucleotide sequences for the deletion of *ben-1*
784 in *P. pacificus*. S14 Table contains all beta-tubulin transcript IDs in the three *Caenorhabditis* species. S15 Table
785 contains the manual curation of SVs found in beta-tubulin genes. S16 Table contains the amino acid sequences
786 for the BEN-1 proteins from the three *Caenorhabditis* species.
787

788 **FUNDING**

789 Amanda O. Shaver was funded by the National Institutes of Health grant F32AI181342. Ryan McKeown was
790 supported by Northwestern University's Biotechnology Training Program (NIH T32 GM008449). This work was
791 supported by the National Institutes of Health grant R01AI153088 to E.C.A.

792 **CRediT AUTHOR STATEMENT**

793 **Conceptualization:** ECA

794 **Data curation:** AOS, RM

795 **Formal analysis:** AOS, RM

796 **Funding acquisition:** ECA

797 **Investigation:** AOS, JMRO, JBC, DWH, JSF, SD, EJR

798 **Methodology:** AOS, RM

799 **Project administration:** ECA

800 **Resources:** ECA

801 **Software:** AOS, RM

802 **Supervision:** ECA

803 **Validation:** AOS, RM

804 **Visualization:** AOS, RM

805 **Writing - original draft:** AOS

806 **Writing - reviewing & editing:** AOS, RM, ECA

807 **DECLARATION OF COMPETING INTERESTS**

808 The authors have declared that no competing interests exist.

809 **ACKNOWLEDGEMENTS**

810 We would like to thank members of the Andersen laboratory for their feedback and helpful comments on this
811 manuscript. We thank members of the *C. elegans* community for collecting the diverse set *Caenorhabditis* strains
812 included in this study and the *Caenorhabditis* Natural Diversity Resource (NSF Capacity grant 2224885) for
813 providing the strains for this study. We thank WormBase for providing the amino acid sequences for all six *C.*
814 *elegans* beta-tubulin proteins [60]. We thank WormBase Parasite for providing the amino acid sequences for
815 TBB-ISOTYPE-1 beta-tubulin protein in *H. contortus* [41].

816 **REFERENCES**

817 1. Kotze AC, Gilleard JS, Doyle SR, Prichard RK. Challenges and opportunities for the adoption of molecular
818 diagnostics for anthelmintic resistance. Int J Forecast. 2020. Available:
819 https://www.sciencedirect.com/science/article/pii/S2211320720300476

820 2. Neff NF, Thomas JH, Grisafi P, Botstein D. Isolation of the beta-tubulin gene from yeast and
821 demonstration of its essential function in vivo. Cell. 1983;33: 211–219.

822 3. Laclette JP, Guerra G, Zetina C. Inhibition of tubulin polymerization by mebendazole. Biochem Biophys
823 Res Commun. 1980;92: 417–423.

824 4. Ireland CM, Gull K, Gutteridge WE, Pogson CI. The interaction of benzimidazole carbamates with
825 mammalian microtobule protein. Biochem Pharmacol. 1979;28: 2680–2682.

826 5. Chalfie M, Thomson JN. Structural and functional diversity in the neuronal microtubules of Caenorhabditis
827 elegans. J Cell Biol. 1982;93: 15–23.

828 6. Theodorides VJ, Scott GC, Lademan MS. Strains of Haemonchus contortus resistant against
829 benzimidazole anthelmintics. Am J Vet Res. 1970;31: 859–863.

830 7. Roos MH, Kwa MSG, Grant WN. New genetic and practical implications of selection for anthelmintic
831 resistance in parasitic nematodes. Parasitol Today. 1995;11: 148–150.

832 8. Beech RN, Prichard RK, Scott ME. Genetic variability of the beta-tubulin genes in benzimidazole-
833 susceptible and -resistant strains of Haemonchus contortus. Genetics. 1994;138: 103–110.

834 9. Sangster NC, Prichard RK, Lacey E. Tubulin and benzimidazole-resistance in Trichostrongylus
835 colubriformis (Nematoda). J Parasitol. 1985;71: 645–651.

836 10. Martínez-Valladares M, Valderas-García E, Gandasegui J, Skuce P, Morrison A, Castilla Gómez de
837 Agüero V, et al. Teladorsagia circumcincta beta tubulin: the presence of the E198L polymorphism on its
838 own is associated with benzimidazole resistance. Parasit Vectors. 2020;13: 453.

839 11. Venkatesan A, Jimenez Castro PD, Morosetti A, Horvath H, Chen R, Redman E, et al. Molecular evidence
840 of widespread benzimidazole drug resistance in Ancylostoma caninum from domestic dogs throughout the
841 USA and discovery of a novel β-tubulin benzimidazole resistance mutation. PLoS Pathog. 2023;19:
842 e1011146.

843 12. Furtado LFV, Dos Santos TR, de Oliveira VNGM, Rabelo ÉML. Genotypic profile of benzimidazole
844 resistance associated with SNP F167Y in the beta-tubulin gene of Necator americanus helminths obtained
845 from Brazilian populations. Infect Genet Evol. 2020;86: 104594.

846 13. Schwenkenbecher JM, Albonico M, Bickle Q, Kaplan RM. Characterization of beta-tubulin genes in
847 hookworms and investigation of resistance-associated mutations using real-time PCR. Mol Biochem
848 Parasitol. 2007;156: 167–174.

849 14. Hahnel SR, Zdraljevic S, Rodriguez BC, Zhao Y, McGrath PT, Andersen EC. Extreme allelic heterogeneity
850 at a Caenorhabditis elegans beta-tubulin locus explains natural resistance to benzimidazoles. PLoS
851 Pathog. 2018;14: e1007226.

852 15. Dilks CM, Hahnel SR, Sheng Q, Long L, McGrath PT, Andersen EC. Quantitative benzimidazole
853 resistance and fitness effects of parasitic nematode beta-tubulin alleles. Int J Parasitol Drugs Drug Resist.
854 2020;14: 28–36.

855 16. Dilks CM, Koury EJ, Buchanan CM, Andersen EC. Newly identified parasitic nematode beta-tubulin alleles

856 confer resistance to benzimidazoles. Int J Parasitol Drugs Drug Resist. 2021;17: 168–175.

857 17. Wit J, Dilks CM, Andersen EC. Complementary Approaches with Free-living and Parasitic Nematodes to
858 Understanding Anthelmintic Resistance. Trends Parasitol. 2021;37: 240–250.

859 18. Saunders GI, Wasmuth JD, Beech R, Laing R, Hunt M, Naghra H, et al. Characterization and comparative
860 analysis of the complete Haemonchus contortus beta-tubulin gene family and implications for
861 benzimidazole resistance in strongylid nematodes. Int J Parasitol. 2013;43: 465–475.

862 19. Silvestre A, Cabaret J. Mutation in position 167 of isotype 1 beta-tubulin gene of Trichostrongylid
863 nematodes: role in benzimidazole resistance? Mol Biochem Parasitol. 2002;120: 297–300.

864 20. Ghisi M, Kaminsky R, Mäser P. Phenotyping and genotyping of Haemonchus contortus isolates reveals a
865 new putative candidate mutation for benzimidazole resistance in nematodes. Vet Parasitol. 2007;144:
866 313–320.

867 21. de Lourdes Mottier M, Prichard RK. Genetic analysis of a relationship between macrocyclic lactone and
868 benzimidazole anthelmintic selection on Haemonchus contortus. Pharmacogenet Genomics. 2008;18:
869 129–140.

870 22. Kwa MS, Veenstra JG, Roos MH. Benzimidazole resistance in Haemonchus contortus is correlated with a
871 conserved mutation at amino acid 200 in beta-tubulin isotype 1. Mol Biochem Parasitol. 1994;63: 299–
872 303.

873 23. Mohammedsalih KM, Krücken J, Khalafalla A, Bashar A, Juma F-R, Abakar A, et al. New codon 198 β-
874 tubulin polymorphisms in highly benzimidazole resistant Haemonchus contortus from goats in three
875 different states in Sudan. Parasit Vectors. 2020;13: 114.

876 24. Kwa MS, Kooyman FN, Boersema JH, Roos MH. Effect of selection for benzimidazole resistance in
877 Haemonchus contortus on beta-tubulin isotype 1 and isotype 2 genes. Biochem Biophys Res Commun.
878 1993;191: 413–419.

879 25. Hurd DD. Tubulins in C. elegans. WormBook. 2018;2018: 1–32.

880 26. Driscoll M, Dean E, Reilly E, Bergholz E, Chalfie M. Genetic and molecular analysis of a Caenorhabditis
881 elegans beta-tubulin that conveys benzimidazole sensitivity. J Cell Biol. 1989;109: 2993–3003.

882 27. Collins JB, Stone SA, Koury EJ, Paredes AG, Shao F, Lovato C, et al. Quantitative tests of albendazole
883 resistance in Caenorhabditis elegans beta-tubulin mutants. Int J Parasitol Drugs Drug Resist. 2024;25:
884 100556.

885 28. Wright AJ, Hunter CP. Mutations in a beta-tubulin disrupt spindle orientation and microtubule dynamics in
886 the early Caenorhabditis elegans embryo. Mol Biol Cell. 2003;14: 4512–4525.

887 29. Ellis GC, Phillips JB, O'Rourke S, Lyczak R, Bowerman B. Maternally expressed and partially redundant
888 beta-tubulins in Caenorhabditis elegans are autoregulated. J Cell Sci. 2004;117: 457–464.

889 30. Lu C, Srayko M, Mains PE. The Caenorhabditis elegans microtubule-severing complex MEI-1/MEI-2
890 katanin interacts differently with two superficially redundant beta-tubulin isotypes. Mol Biol Cell. 2004;15:
891 142–150.

892 31. Pallotto LM, Dilks CM, Park Y-J, Smit RB, Lu BT, Gopalakrishnan C, et al. Interactions of Caenorhabditis
893 elegans β-tubulins with the microtubule inhibitor and anthelmintic drug albendazole. Genetics. 2022;221.
894 doi:10.1093/genetics/iyac093

895 32. Boulin T, Etchberger JF, Hobert O. Reporter gene fusions. WormBook. 2006; 1–23.

896 33. Gibson SB, Ness-Cohn E, Andersen EC. Benzimidazoles cause lethality by inhibiting the function of
897 Caenorhabditis elegans neuronal beta-tubulin. Int J Parasitol Drugs Drug Resist. 2022;20: 89–96.

898 34. Hahnel, Dilks, Heisler, Andersen. Caenorhabditis elegans in anthelmintic research–Old model, new
899 perspectives. Int J Educ Vocat Guid. 2020. Available:
900 https://www.sciencedirect.com/science/article/pii/S2211320720300312

901 35. Mariene GM, Wasmuth JD. Genome assembly variation and its implications for gene discovery in
902 nematodes. Int J Parasitol. 2025. doi:10.1016/j.ijpara.2025.01.004

903 36. Crombie TA, McKeown R, Moya ND, Evans KS, Widmayer SJ, LaGrassa V, et al. CaeNDR, the
904 Caenorhabditis Natural Diversity Resource. Nucleic Acids Res. 2023. doi:10.1093/nar/gkad887

905 37. Shaver AO, Miller IR, Schaye ES, Moya ND, Collins JB, Wit J, et al. Quantifying the fitness effects of
906 resistance alleles with and without anthelmintic selection pressure using Caenorhabditis elegans. PLoS
907 Pathog. 2024;20: e1012245.

908 38. Zhang G, Roberto NM, Lee D, Hahnel SR, Andersen EC. The impact of species-wide gene expression
909 variation on Caenorhabditis elegans complex traits. Nat Commun. 2022;13: 3462.

910 39. Henikoff S, Henikoff JG. Amino acid substitution matrices from protein blocks. Proc Natl Acad Sci U S A.
911 1992;89: 10915–10919.

912 40. Grantham R. Amino acid difference formula to help explain protein evolution. Science. 1974;185: 862–
913 864.

914 41. Howe KL, Bolt BJ, Shafie M, Kersey P, Berriman M. WormBase ParaSite - a comprehensive resource for
915 helminth genomics. Mol Biochem Parasitol. 2017;215: 2–10.

916 42. Large CRL, Khanal R, Hillier L, Huynh C, Kubo C, Kim J, et al. Lineage-resolved analysis of embryonic
917 gene expression evolution in *C. elegans* and *C. briggsae*. Science. 2025;388: eadu8249.

918 43. Toker IA, Ripoll-Sánchez L, Geiger LT, Sussfeld A, Saini KS, Beets I, et al. Divergence in neuronal
919 signaling pathways despite conserved neuronal identity among Caenorhabditis species. Curr Biol.
920 2025;35: 2927–2945.e7.

921 44. Andersen EC, Gerke JP, Shapiro JA, Crissman JR, Ghosh R, Bloom JS, et al. Chromosome-scale
922 selective sweeps shape Caenorhabditis elegans genomic diversity. Nat Genet. 2012;44: 285–290.

923 45. Zhang G, Mostad JD, Andersen EC. Natural variation in fecundity is correlated with species-wide levels of
924 divergence in Caenorhabditis elegans. G3 . 2021;11. doi:10.1093/g3journal/jkab168

925 46. Laing ST, Ivens A, Laing R, Ravikumar S, Butler V, Woods DJ, et al. Characterization of the xenobiotic
926 response of Caenorhabditis elegans to the anthelmintic drug albendazole and the identification of novel
927 drug glucoside metabolites. Biochem J. 2010;432: 505–514.

928 47. Collins JB, Dilks CM, Hahnel SR, Rodriguez B, Fox BW, Redman E, et al. Naturally occurring variation in
929 a cytochrome P450 modifies thiabendazole responses independently of beta-tubulin. PLoS Pathog.
930 2025;21: e1012602.

931 48. Athanasouli M, Witte H, Weiler C, Loschko T, Eberhardt G, Sommer RJ, et al. Comparative genomics and
932 community curation further improve gene annotations in the nematode Pristionchus pacificus. BMC
933 Genomics. 2020;21: 708.

934 49. Doyle SR, Tracey A, Laing R, Holroyd N, Bartley D, Bazant W, et al. Genomic and transcriptomic variation
935 defines the chromosome-scale assembly of Haemonchus contortus, a model gastrointestinal worm.

936 Commun Biol. 2020;3: 656.

937 50. Doyle SR. Improving helminth genome resources in the post-genomic era. Trends Parasitol. 2022 [cited 4
938 Jul 2022]. Available: https://pubag.nal.usda.gov/catalog/7806127

939 51. Montarry J, Mimee B, Danchin EGJ, Koutsovoulos GD, Ste-Croix DT, Grenier E. Recent Advances in
940 Population Genomics of Plant-Parasitic Nematodes. Phytopathology. 2021;111: 40–48.

941 52. Stevens L, Moya ND, Tanny RE, Gibson SB, Tracey A, Na H, et al. Chromosome-level reference
942 genomes for two strains of Caenorhabditis briggsae: An improved platform for comparative genomics.
943 Genome Biol Evol. 2022;14. doi:10.1093/gbe/evac042

944 53. Moya ND, Stevens L, Miller IR, Sokol CE, Galindo JL, Bardas AD, et al. Novel and improved
945 Caenorhabditis briggsae gene models generated by community curation. BMC Genomics. 2023;24: 486.

946 54. Luke M, Noble J, Yuen L, Stevens N, Moya R. Selfing is the safest sex for Caenorhabditis tropicalis. eLife.
947 2021;10.

948 55. Geldhof P, Murray L, Couthier A, Gilleard JS, McLauchlan G, Knox DP, et al. Testing the efficacy of RNA
949 interference in Haemonchus contortus. Int J Parasitol. 2006;36: 801–810.

950 56. Roose S, Avramenko RW, Pollo SMJ, Wasmuth JD, Ame S, Ayana M, et al. Characterization of the β-
951 tubulin gene family in Ascaris lumbricoides and Ascaris suum and its implication for the molecular
952 detection of benzimidazole resistance. PLoS Negl Trop Dis. 2021;15: e0009777.

953 57. Krücken J, Fraundorfer K, Mugisha JC, Ramünke S, Sifft KC, Geus D, et al. Reduced efficacy of
954 albendazole against Ascaris lumbricoides in Rwandan schoolchildren. Int J Parasitol Drugs Drug Resist.
955 2017;7: 262–271.

956 58. Palma A, Matamoros G, Escobar D, Sánchez AL, Fontecha G. Absence of mutations associated with
957 resistance to benzimidazole in the beta-tubulin gene of Ascaris suum. Rev Soc Bras Med Trop. 2020;53:
958 e20190155.

959 59. Collins JB, Andersen EC. The turkey ascarid, Ascaridia dissimilis, as a model genetic system. Int J
960 Parasitol. 2023;53: 405–409.

961 60. Sternberg PW, Van Auken K, Wang Q, Wright A, Yook K, Zarowiecki M, et al. WormBase 2024: status
962 and transitioning to Alliance infrastructure. Genetics. 2024;227. doi:10.1093/genetics/iyae050

963 61. Camacho C, Coulouris G, Avagyan V, Ma N, Papadopoulos J, Bealer K, et al. BLAST+: architecture and
964 applications. BMC Bioinformatics. 2009;10: 421.

965 62. Noble LM, Yuen J, Stevens L, Moya N, Persaud R, Moscatelli M, et al. Selfing is the safest sex for
966 Caenorhabditis tropicalis. eLife. 2021. doi:10.7554/elife.62587

967 63. Pertea G, Pertea M. GFF utilities: GffRead and GffCompare. F1000Res. 2020;9: 304.

968 64. Rausch T, Zichner T, Schlattl A, Stütz AM, Benes V, Korbel JO. DELLY: structural variant discovery by
969 integrated paired-end and split-read analysis. Bioinformatics. 2012;28: i333–i339.

970 65. Lesack K, Mariene GM, Andersen EC, Wasmuth JD. Different structural variant prediction tools yield
971 considerably different results in Caenorhabditis elegans. PLoS One. 2022;17: e0278424.

972 66. Danecek P, Bonfield JK, Liddle J, Marshall J, Ohan V, Pollard MO, et al. Twelve years of SAMtools and
973 BCFtools. Gigascience. 2021;10. doi:10.1093/gigascience/giab008

974 67. Shaver AO, Wit J, Dilks CM, Crombie TA, Li H, Aroian RV, et al. Variation in anthelmintic responses are

975 driven by genetic differences among diverse C. elegans wild strains. PLoS Pathog. 2023;19: e1011285.

976 68. Ortiz EM. vcf2phylip v2.0: convert a VCF matrix into several matrix formats for phylogenetic analysis.
977 Zenodo; 2019. doi:10.5281/ZENODO.2540861

978 69. Caro H, Dollin S, Biton A, Brancotte B, Desvillechabrol D, Dufresne Y, et al. BioConvert: a comprehensive
979 format converter for life sciences. NAR Genom Bioinform. 2023;5: lqad074.

980 70. Saitou N, Nei M. The neighbor-joining method: a new method for reconstructing phylogenetic trees. Mol
981 Biol Evol. 1987;4: 406–425.

982 71. Yu G. Using ggtree to Visualize Data on Tree-Like Structures. Curr Protoc Bioinformatics. 2020;69: e96.

983 72. Andersen EC, Bloom JS, Gerke JP, Kruglyak L. A variant in the neuropeptide receptor npr-1 is a major
984 determinant of Caenorhabditis elegans growth and physiology. PLoS Genet. 2014;10: e1004156.

985 73. Andersen EC, Shimko TC, Crissman JR, Ghosh R, Bloom JS, Seidel HS, et al. A Powerful New
986 Quantitative Genetics Platform, Combining Caenorhabditis elegans High-Throughput Fitness Assays with
987 a Large Collection of Recombinant Strains. G3 . 2015;5: 911–920.

988 74. Zamanian M, Cook DE, Zdraljevic S, Brady SC, Lee D, Lee J, et al. Discovery of genomic intervals that
989 underlie nematode responses to benzimidazoles. PLoS Negl Trop Dis. 2018;12: e0006368.

990 75. Widmayer SJ, Crombie TA, Nyaanga JN, Evans KS, Andersen EC. C. elegans toxicant responses vary
991 among genetically diverse individuals. Toxicology. 2022; 153292.

992 76. Shaver A, Andersen E. High-throughput larval development assay (HTLDA) v1. 2025.
993 doi:10.17504/protocols.io.n92ldrqwng5b/v1

994 77. Nyaanga J, Crombie TA, Widmayer SJ, Andersen EC. easyXpress: An R package to analyze and
995 visualize high-throughput C. elegans microscopy data generated using CellProfiler. PLoS One. 2021;16:
996 e0252000.

997 78. Wählby C, Kamentsky L, Liu ZH, Riklin-Raviv T, Conery AL, O'Rourke EJ, et al. An image analysis toolbox
998 for high-throughput C. elegans assays. Nat Methods. 2012;9: 714–716.

999 79. Wang C, Vidal B, Sural S, Loer C, Aguilar GR, Merritt DM, et al. A neurotransmitter atlas of C. elegans
000 males and hermaphrodites. Elife. 2024;13. doi:10.7554/elife.95402.3

001 80. Abramson J, Adler J, Dunger J, Evans R, Green T, Pritzel A, et al. Accurate structure prediction of
002 biomolecular interactions with AlphaFold 3. Nature. 2024;630: 493–500.

003 81. Han Z, Lo W-S, Lightfoot JW, Witte H, Sun S, Sommer RJ. Improving transgenesis efficiency and
004 CRISPR-associated tools through Codon optimization and native intron addition in Pristionchus
005 nematodes. Genetics. 2020;216: 947–956.